Desalination and Water Treatment
www.deswater.com

doi: 10.5004/dwt.2021.26672

213 (2021) 1–25
February

Treatment of highly saline brines using a static freeze crystallisation process

Mansour Ahmed[a,*], Darren Oatley-Radcliffe[b], Paul M. Williams[b]

[a]*Water Research Center, Kuwait Institute for Scientific Research, P.O. Box: 24885, 13109 Safat, Kuwait, email: mahmed@kisr.edu.kw*
[b]*Centre for Water Advanced Technologies and Environmental Research (CWATER), College of Engineering, Swansea University, Bay Campus, Swansea SA2 8EN, UK, emails: d.l.oatley@swansea.ac.uk (D. Oatley-Radcliffe), paul.melvyn.williams@swansea.ac.uk (P.M. Williams)*

Received 3 August 2020; Accepted 14 October 2020

ABSTRACT

Pilot and semi-pilot plants using the static freeze crystallisation process were investigated for concentrating reverse osmosis (RO) brines with different salinities. The pilot plant results revealed that the crystallisation experiments (without a sweating process) operating at a temperature of –4°C achieved a permeate concentration and water recovery ratio of 3.46 wt.% and 73%, respectively, indicating permeate of near ocean seawater standards. As a result, the treated water can be further desalted by the seawater RO plant. As for the case of concentrated RO brine (9.78 wt.%), a semi-pilot plant using feed stage with and without the sweating process was assessed. Before performing the sweating process, the results showed that the permeate concentration was reduced from 9.78 to 8.40 wt.% by decreasing the cooling rate of the crystallisation process from –0.80 to –0.48°C/min. For the case of the crystallisation rate of –0.80°C/min with the sweating process, the permeate concentration was reduced from 9.78 to 4.50 wt.% when the crystal mass ratio reached 35.64%. For the case of the crystallisation rate of –0.48°C/min, the permeate salinity was further reduced by the sweating process, where the permeate concentration was lowered from 8.40 to 3.68 wt.% when the crystal mass ratio reached 36.25%. In general, the salt rejection ratio increased whereas the water recovery ratio decreased as the cooling rate, crystal mass ratio, and sweating time increased.

Keywords: Freeze-melting process; Freezing desalination technologies; Melt crystallisation process; Reverse osmosis (RO) concentrate; RO retentate

1. Introduction

Freeze desalination is a freezing–melting (FM) process in which freshwater is crystallized to ice crystals and separated from the saline water. It is an alternative physical process, which can be utilized for desalination applications. Freeze desalination technologies involve three main stages including: crystallisation, ice washing, and ice melting to recover fresh water. Previous studies have reported that this technology is effective for removing various organic and inorganic contaminants from water and wastewater [1–3]. There are two main types of FM methods that are available: (i) suspension melt freeze crystallisation and (ii) solid-layer freeze crystallisation (or progressive freeze crystallisation).

The fact that freeze-melting can purify and concentrate liquids has been known for many years, with the first recorded examples of the process being in the 1600's [4]. Nebbia and Menozzi [4] reported that the first published paper for water desalination by freezing was introduced by Antonio Maria Lorgna (1735–1796) in 1786. Lorgna carried out the first experiments on desalination by freezing, by producing a block of freshwater ice from seawater. However, before the development of refrigeration systems, the proposed treatment system was not practical and was limited

* Corresponding author.

to the coldest regions and seasons. According to Nebbia and Menozzi [4], the first experimental freezing desalination plant was developed in the late 1930's in Italy by the Institute Superior di Sánita. This desalination plant was operated using the indirect freezing process [4]. According to Johnson [5], the first successful pilot plant was demonstrated by the Carrier Corporation. This plant used a vacuum freeze process employing an absorption system. Another company, known as the Struthers Wells Corporation (USA), was heavily involved in developing a secondary refrigerant freeze technology. A plant with a capacity of 200,000 gpd was built during the early 1960 s [5]. Colt Industries, on the other hand, continued the development of a primary vacuum freeze process, and successfully constructed a pilot plant with a capacity of 100,000 gpd at Wrightsville Beach, North Carolina (USA), in the late 1960s. The plant was tested over 2,000 h of operation, and the power consumption was around 10.34 kWh/m^3, which was encouraging for a non-optimised pilot plant [5]. The United Kingdom Atomic Energy Authority (UKAEA) (England) in cooperation with Simon Carves (England), which is a commercial organisation, developed a secondary refrigerant process with a plant capacity of 10,000 gpd [5]. The investigated plant was successfully operated, and the results were encouraging enough to scale up the plant capacity to 1 MGD and was to be constructed at Ipswich (England), but was then rejected [5]. In addition to these plants, several freezing desalination plants were built for the purpose of creating drinking water. A pilot plant using vacuum freezing vapour compression technology was constructed in Middle East; while another plant, utilizing secondary refrigerant freezing, was built in Florida (USA); and a pilot plant, using an indirect freezing process, was built in Yanbu (Saudi Arabia) [6]. Several approaches using freezing desalination technologies were developed in the period 1950–1970 [7]. The classification of the different freeze-melting (FM) processes can be divided into three concepts based on contact of refrigerant with the solution: direct contact freezing, indirect contact freezing, and vacuum freezing [7,8]. The most commonly known technologies are indirect freezing processes with a secondary refrigerant, vacuum-freezing vapour compression process, vacuum-freezing vapour absorption process, and secondary refrigerant freezing process.

From an industrial separation viewpoint, the best potential advantages of freezing desalination technologies are as follows: (i) freezing desalination technologies, in theory, require less energy when compared with the evaporation/distillation process, because the latent heat of fusion of ice is only one-seventh the latent heat of vaporisation of water [9,10]. Therefore, theoretically, desalination by freezing could achieve a 75%–90% reduction in the energy required by a conventional thermal process [10]; (ii) the energy cost of a freezing desalination process is theoretically almost similar to that of an RO membrane plants; however, the investment and operational costs for freezing technologies are less than RO membrane plants, because the biological fouling is substantially reduced by low-temperature operation [9,10]; (iii) the advantages of a low operating temperature minimises the major technical problems, such as scaling and corrosion, that are usually encountered in thermal desalination plants [7,10]; (iv) the low operating temperature can minimise the capital cost, because many inexpensive plastics or low-cost materials can be utilised at low temperature [7–10]; (v) the freezing desalination technologies require very low chemical use due to the absence of pre-treatment systems, and therefore this process is environmentally-friendly, because there is no discharge of toxic chemicals to the surrounding environment [10]; (vi) by using direct contact freezing desalination technology, a very high surface area and high heat transfer coefficient can be achieved [10]; (vii) freezing desalination process is insensitive to the nature of feed stream in terms of salinity or type of substances in the feed water [7–10].

Despite these advantages, the FM process has been used only to a very limited extent industrially, especially for seawater applications. Commercially, the FM process has not achieved the success of other conventional processes for seawater applications, because of the process complexity and the prohibitive total cost compared with conventional membrane and distillation technologies [10]. In general, the disadvantages and main reasons behind restricting the application of freezing desalination plants are as follows [10]: (i) freezing desalination requires complicated equipment to deal with growing, handling, washing, and melting ice crystals; (ii) the final product may be produced with undesirable flavour and aroma; (iii) the freezing technologies require mechanical vapour compressors; (iv) large-scale compressors intensively consume energy when used in desalination; (v) difficulties in designing large-scale plant using freezing desalination technologies and optimising the operating conditions with confidence, because of the process and operation units complexity in the main equipment of the freezing desalination plants, such as freezing chamber, and separation and melting units; Impure ice crystals are usually produced due to adherence of drops or pockets of the reject brine. As a result, crushing and re-crystallisation of ice may be needed; (vi) progressive increases in the salinity of reject brine and non-condensable gases; (vii) high-quality energy is essential for freezing desalination technologies, while many evaporation processes can be applied with low-quality energy; (viii) mass loss in product water due to certain amount of fresh water taken as wash liquor for washing the ice crystal in the separation unit; (ix) lack of knowledge on ice crystallisation and growth in a slurry system, and limited knowledge in handling ice slurries and separation of ice from brine.

To date, a commercial application of freezing desalination technology processes does not exist. However, a similar concept, in terms of the freeze-melting process, is widely available for use in many different industrial sectors, particularly in food processing [11–15]. Rahman et al. [8] illustrated various commercial food applications that utilise freeze-melting technologies, which are known as melt crystallisation processes. The solid layer and suspension crystallisation processes are widely used, for such applications. The crystallisers being used in these technologies are classified as indirect contact crystallisers, where the food and refrigerant are fully separated by heat transfer walls and surfaces [8]. The most commonly used crystallisation techniques are: static crystallisation, layer crystallisation growing on a rotating drum, dynamic crystallisation, and suspension crystallisation [8]. The food industries use

the principles that could be applied to freeze desalination technologies and have taken advantage of the technology [8]. In fact, melt crystallisation processes in food industries achieved great success due to the ability of producing high-quality products compared with other available technologies around the world [8].

Desalination, however, is a massively important process due to the high-water usage across the globe, and the constant necessity for clean water [8,16,17]. According to Ulrich and Glade [18], the important advantages of solid-layer crystallisation technologies are (i) no incrustation problems, as these incrustations represent the solid layer, which will eventually be separated, melted, and recovered as final product water; (ii) easily controllable crystal growth rates, due to the driving force being dependant on the temperature difference at the refrigerated surface area of the plate; (iii) a simplified separation process due to absence of an ice slurry. Thus, complicated ice separation and washing equipment, usually used in conventional desalination through freezing processes and melt suspension crystallisation technologies, are avoided. Furthermore, no moving parts are involved in the process equipment (apart from circulation pump); (iv) the operation of the post-crystallisation treatments, such as washing and sweating, is simple; and (v) multistage process design can easily be applied. On the other hand, the limitations of these technologies are summarised in four main points. According to Ulrich and Glade [18], (a) the surface area of the refrigerated plate is limited; (b) the crystal layer adhered on the heat transfer surface requires an increase in temperature driving force to maintain the constant growth rate; otherwise a reduction in production rate will occur with increasing thickness; (c) the crystallisation and post-crystallisation operations are limited in batch operating mode. This is because the desired crystal layer has to be completely melted and separated from the crystalliser, before starting the subsequent crystallisation operations. This method requires additional energy for the melting process and partial heating up of the whole apparatus. (d) In the case of a multistage process, the operational cost is dramatically increased due to the repetition of the crystallisation process, while the production rate of the overall multistage process is decreased. The last two points may be avoided at some point, when the solid-layer crystallisation technology is operated in continuous mode.

Solid-layer crystallisation technologies, more specifically the static freeze crystallisation (SFC) process, are however potentially capable of further concentrating highly saline brines. The majority of previous studies on the SFC technology has focused on process design and operation to improve the efficiency of crystalline layers in terms of purity and yield [18]. These studies have concentrated on different vital applications including pharmaceuticals, and chemical and food processing [18]. However, there is a marked absence of research and development in the scope of RO brine treatment and concentration.

In this paper, a Sulzer SFC laboratory bench-scale test unit and an industrial pilot-scale plant were used in order to test the process for desalination of different types of feed solutions. According to Sulzer's experts, this technology has not previously been examined or applied to treating concentrated solutions of RO brine. The main objective of this study is to determine the viability and assess the technical feasibility of using static crystallisation and sweating processes to produce final product water (either close to the quality of seawater or RO retentate) by concentrating the residues discharged from prior processes, such as the falling film and the suspension crystallisation processes. Details of the prior processes are available in the literature [19,20]. Along with concentrated solutions of prior processes, Arabian Gulf seawater, and NaCl solutions were individually tested as feed water in this study. Effect of several key parameters, including feed salt concentration, crystallisation time and temperature, sweating time and temperature, cooling rate, and growth rate, on the performance of the static crystallisation and sweating processes, in terms of salt rejection and water recovery, were investigated. In addition to this, the separation efficiency, under the influence of the SFC and sweating operations, in rejecting major components of ionic concentration (e.g., Ca^{2+}, Mg^{2+}, $(SO_4)^{2-}$, $(HCO_3)^-$, Cl^-, Na^+, etc.) for the investigated solutions was evaluated. This investigation represents the first laboratory examination to successfully gather valuable, quantitative information concerning the separation performance of the proposed technology in such applications.

2. Materials and methods

2.1. Description of the static crystallisation process apparatus and basic operation

The SFC process, which was investigated in this study, is characterised as a stagnant melt with the use of forced convection principles, in batch operating mode. The Sulzer static crystalliser differs from conventional static crystallisers in that it utilises a vertical plate heat exchanger type rather than a tube-type heat exchanger, as shown in Fig. 1. The vertical plate is immersed inside a tank filled with a stagnant melt, enabling the crystal layer to nucleate and grow on a cooled exterior surface of the heat exchanger. The latter is cooled and heated by means of internal circulation of a heat transfer medium (HTM). The operating conditions of the HTM are managed and controlled via a PID temperature controller of the refrigeration system.

A typical example of the commercial crystalliser, using Sulzer's SFC process, is illustrated in Fig. 2, and consists of a sealed tank, number of vertical plate heat exchangers, melt inlet and outlet, and HTM inlet and outlet.

As shown schematically in Fig. 2, the vertical plate heat exchanger is placed inside a tank, where both represent a crystalliser. The latter is provided with a HTM refrigeration unit along with a PID temperature controller. The principles of the Sulzer SFC process are described in more detail in the literature [18,21]. Sulzer have developed over 200 applications since starting efforts in this field [18]. The technology used in this article is the SFC process which is most commonly used in the separation of organic materials ranging from isomer separation to tar chemical mixtures, and from organics acid to monomers [18,21]. Table 1 shows the comparison of the characteristics of the solid crystal layer and suspension crystallisation processes.

The main phases of the Sulzer SFC process are six successive processes, namely (i) filling, (ii) pre-cooling,

(iii) nucleation, (iv) crystallisation, (v) partial melting (sweating), and (vi) melting. Fig. 3 shows the process set-point HTM temperature vs. the running time of a complete freezing stage. The major phases of the Sulzer SFC technology, such as crystallisation, draining, sweating, and melting, are also illustrated in Fig. 3. The set-points temperature and time of these phases is controlled through a PID temperature controller driving the refrigeration system.

The SFC process is applied under a non-adiabatic environment and operated under atmospheric pressure [22]. The principles of operation of this technology are briefly described below:

2.1.1. Filling process

The crystalliser is filled with the desired mass of feed by opening the melt inlet valve, enabling the melt to flow into the crystalliser through a melt inlet line as shown in Fig. 2b. When the crystalliser is completely loaded with the predetermined amount of feed, then the melt inlet valve is closed.

Fig. 1. Plate-type heat exchanger used in the commercial Sulzer static crystalliser.

2.1.2. Pre-cooling

By passing cold HTM into each vertical plate heat exchanger, the HTM absorbs heat from the melt through the refrigerated surfaces of the plate heat exchanger, and consequently, the temperature of the melt is slowly reduced. By continuously circulating the cold HTM around a plate heat exchanger, the temperature of the melt is lowered until it reaches the predetermined temperature of the melt, which is slightly lower than the freezing point of the feed.

2.1.3. Nucleation

Once the temperature of the melt reaches the predetermined temperature, a seed ice crystal is usually added to achieve nucleation of ice crystals, which then grow gradually on the heat transfer surface during the crystallisation process.

2.1.4. Crystallisation

When the cold HTM is continuously circulated in a plate heat exchanger, a uniform crystal layer is allowed to grow and build up as an ice slab on the heat exchanger refrigerated surface. By operating the crystallisation step with a linear cooling ramp, the temperature of the flowing HTM is linearly reduced over the running time of the crystallisation process. The variation of the temperature of the HTM, as a function of the crystallisation time, is shown in Fig. 3. As the thickness of the ice slab increases, the impurities are rejected from the growing crystal layer, and are gradually concentrated in the remaining melt [18]. When the predetermined crystallisation time is reached, the crystallisation process is deactivated and the residue is collected from the

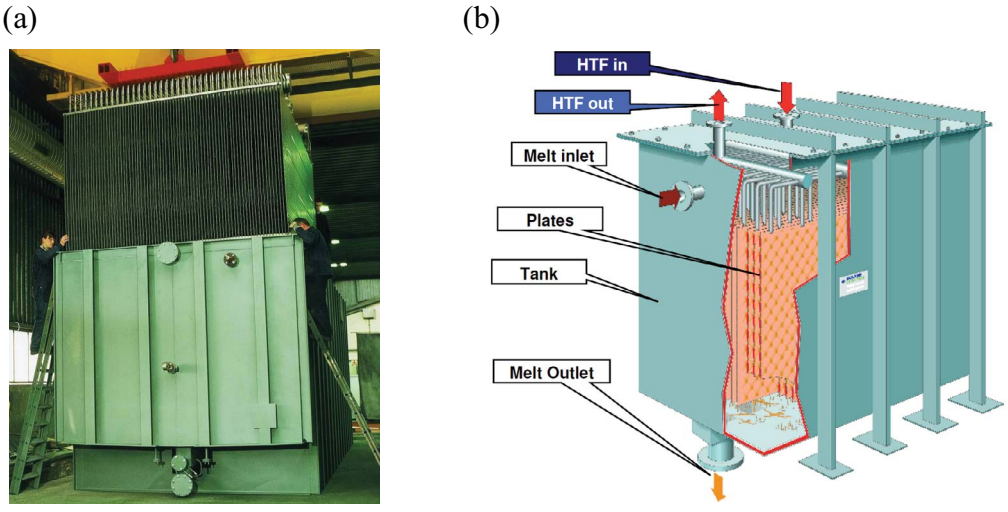

Fig. 2. Sulzer commercial static crystalliser [18,21] (a) Sulzer static crystallizer and (b) schematic diagram of static crystalliser.

Table 1
General comparison of the characteristics of the solid crystal layer and suspension crystallisation processes [18]

Feature	Crystallisation process	
	Solid crystal layer	Suspension
Process concept	Based on the formation of a crystal layer on a cooled heat exchanger	Based on the formation of crystals which are freely suspended in the mother liquor
Process equipment	No moving parts except HTM circulation pump for the static crystallisation process (and melt circulation pump, stirrer, air-pump, ultrasonic device for the dynamic crystallisation processes)	Moving parts (e.g., circulation pumps, scrapers, piston drive)
Operation	Discontinuous (predominantly)	Continuous (predominantly)
Washing equipment	Partial melting (sweating) or rinsing	Piston-type wash-column
Temperature of melt	Close to above solidification temperature	Below solidification temperature
Melt flow-rate	• Low for static crystallisation • High for falling film crystallisation	Low
Heat withdraw	Through crystal layer	Through the melt
Crystal growth rate	High	Low
Relative interface crystal-melt	Low	High
Product transportation	Simple	Difficult
Solid–liquid separation	Simple	Difficult
Encrustation problems	No	Accessible (removed continuously by scraper)
Scale-up	Simple	Difficult
Energy consumption	High	Low

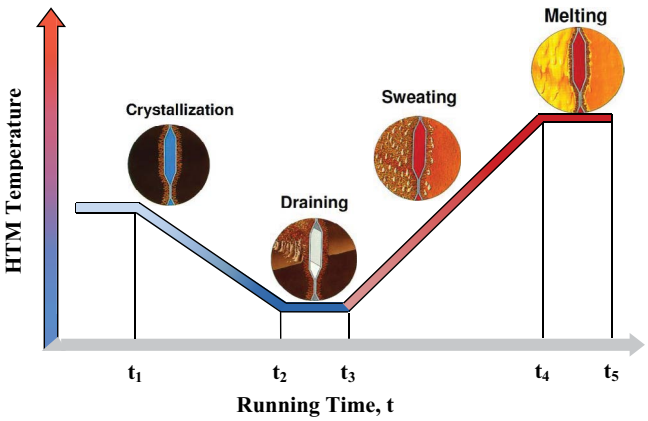

Fig. 3. Process set-point temperature-time profile [18,21].

crystalliser through the melt outlet line (Fig. 2b). The residue is then either taken to the drain discharge or to an intermediate storage vessel for performing a multistage operation.

2.1.5. Partial melting (sweating)

The sweating process is defined as a temperature-induced purification step based on a partial melting process achieved by gradually increasing the temperature of the crystalliser up to a certain level close to the freezing point of the required product [18]. Thus, considerable amounts of impurities adhering within the crystal surface of the crystalline and those brine buckets, contained in pores of the crystalline structure, can be removed and drained under the influence of gravity [18]. During the sweating process, the rejected brines adhering to the crystal surface and those contained within the pores of the crystalline will be partially diluted with pure water melted. Then, the diluted brines will be drained under the influence of the gravity. The temperature increase along with the sweating step simultaneously reduces the viscosity of the residual liquids and thus further facilitates the draining process [18]. Therefore, the sweating process can improve the purity of ice crystals. On completion of removing the residue, the partial melting process (i.e., sweating phase) is activated by gradually increasing the temperature of the flowing heating medium into the crystalliser through a HTM conditioning unit. Consequently, the wall of the crystalliser is heated gradually to induce partial melting. The melted ice (i.e., sweat fraction) is drained off or transported either to the respective storage vessel or intermediate storage vessel for a subsequent purification step in multistage operation. This means that the residue can be further treated by recycling the sweat fraction into the intermediate feed or residue vessel to be used as a feedstock and repeating the previous steps.

2.1.6. Melting

The melting process is operated by increasing the temperature of the heating medium through a HTM conditioning unit. Consequently, the remaining crystal layer is melted and collected as either product or transported into

the intermediate storage vessel for a subsequent purification step in multistage operation.

2.2. Multi-stage design and basic operation

Based on the end-user demand, the degree of purity and/or concentration can be achieved with a single crystalliser by using the intermediate vessel as a feed and repeating the freezing process [18,21]. This means that the product and reject of the first stage will be individually used once more as feed in the second freezing stage for achieving further treatment process. For the case of Sulzer commercial plants, the number of freezing stages can be varied between one and seven stages [18,21]. These stages can be performed in a multi-stage method by using a single crystalliser using a batch method. By using a single crystalliser, the capital and operational expenses will be drastically reduced, however, this option may be limited by a number of aspects, including plant capacity [21]. As an example of multi-stage design, Fig. 4 shows the mass flow in a three-stage process, namely feed, rectification, and stripping stages [18,21]. The first freezing stage is considered as the feed stage, which is mainly used for purifying and concentrating the product and brine, respectively [18,21]. The rectification and stripping stages are the repeated freezing stages for purifying and concentrating the product and the brine, respectively [18,21].

2.3. Preparation of feed samples

Arabian Gulf seawater, reverse osmosis (RO) brine and aqueous solutions of sodium chloride were used and tested as feed samples in this experimental study. Sodium chloride (CH-4133 Pratteln 1, Nr.: 8431, BAGT 64656, Schweizer Rheinsalinen) and high purity water, produced via an ultra-pure water purification system (Destillo, Einweg-Patrone D2), were used for preparing the aqueous solutions of sodium chloride. The feed samples were prepared by dissolving a predetermined mass of NaCl into a known mass of deionised water. The initial salt concentration of the aqueous solutions used was 3.5 wt.%. As for the process brines, Arabian Gulf seawater and RO brine were used and examined individually as feed samples in this study. The principles of RO membrane technologies, including the description of reject brines, are described elsewhere [7,23,24]. The investigated Arabian Gulf seawater and RO brine were collected from the feed stream and reject brine discharge of the Kadhmah Bottled Water plant in Kuwait. Table 2 summarises the results of the major physiochemical characteristics of the tested samples. Alongside the seawater and RO brine, the residual liquids discharged from falling film and suspension crystallisation processes were also collected and tested as feed water in this study. It is important to state that there are a series of previous studies conducted by the authors on the falling film and suspension crystallisation technologies for desalination of seawater and RO brine which provided these feeds [19,20].

2.4. Physicochemical analysis and measuring instruments

Upon collection of feed samples, physicochemical analysis was performed for the collected sample. After completion of each experiment, the physiochemical analysis was then carried out for the product and residue samples. The physiochemical analysis of water samples included measurements of the temperature, total dissolved solids (TDS), electrical conductivity, pH, volume, and weight. Two different types of measurements of salt concentration are considered in the physiochemical analysis to cross-check the reliability of the results. They are as follows: (i) electrical conductivity and (ii) gravimetric method. In addition

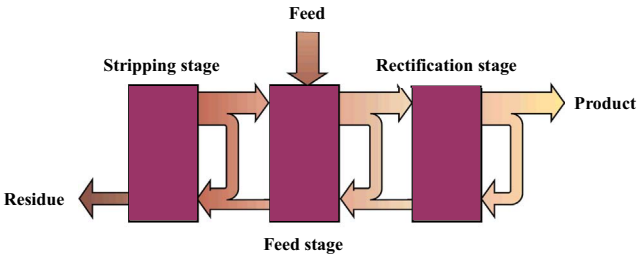

Fig. 4. Mass flows in a three-stage process [18,21].

Table 2
Summary of major physiochemical analysis of the tested water samples

Parameters	Water samples	
	Arabian Gulf seawater	RO brine
Salt concentration, wt.%	4.91	6.11
Salt concentration, mg/L	49,074	61,104
Electrical conductivity, mS/cm	63.6	76.6
Freezing point, °C	–2.52	–3.1
Ca^{2+}, mg/L	1,080	1,476
Mg^{2+}, mg/L	1,387	1,463
Na^{+}, mg/L	16,523	20,880
Cl^{-}, mg/L	25,480	32,200
$(HCO_3)^{-}$, mg/L as $CaCO_3$	175.6	241.2
$(SO_4)^{2-}$, mg/L	3,900	4,800

to this, the accuracy of salt concentration measurements (which are obtained by a gravimetric method) was also ensured by means of a simple mass balance equation. In addition, full water chemistry analysis was performed for all samples of each experiment. The purpose of conducting full water chemistry analysis is to detect the major components of ionic composition found in the feed, product, and residue. The reliability of full chemical analysis of the water samples was ensured by using a charge balance error. Furthermore, the salinity, in term of TDS, was also ensured by comparing the results of TDS obtained through physicochemical analysis and gravimetric method. In addition, the measurements of freezing point were covered in this investigation. Furthermore, the temperature profiles and running times of the pre-cooling, crystallisation, partial melting, total melting, and freezing stage of each test were monitored and recorded. However, the pH measurements were not considered in this study. The physicochemical analysis of water samples was performed experimentally using the measuring instruments, auxiliary equipment, tools, and laboratory facilities of Sulzer Chemtech Ltd. (Buchs SG, Switzerland). For further investigation and cross checking, several sets of water samples were sent to two different laboratories at Kuwait Institute for Scientific Research (KISR, Kuwait) namely Desalination Research Plant laboratory and the Central Analytical Laboratories for performing similar chemical analysis and also carrying out full chemical analyses on water samples to detect the major ionic composition. Results of these measurements are tabulated in the Results and Discussion section.

The salt concentration of the feed sample was measured via a conductivity meter (Cond 3110, TetraCon® 325) and a conductivity probe (Conductivity probe model: TetraCon 325, Wissenschaftlich-Technische Werkstätten GmbH, Germany) to ensure that the correct concentration was achieved. The measurements of TDS were experimentally determined, using the gravimetric method, by evaporating a known weight of water sample to dryness, and weighing the solid residue. The equipment involved in obtaining gravimetric measurements are as follows: oven (Heraeus Instruments, Type: UT 12P, D-63450 Hanau, Kendro Laboratory Products, USA), Petri dish, and laboratory balance (Mettler Toledo PM 460, Delta Range, CH-8606, USA). The accuracy of salt concentration results was assured through a simple mass balance equation. The volume and weight measurements, on the other hand, were determined by a laboratory beaker, scaled borosilicate glass cylinder (Barcode: CYL-350-020J, Fisher Scientific, USA) and a laboratory balance (Mettler Toledo, Model: PM30-K, USA). The running time for the crystallisation process was measured by a stopwatch timer (HS-10W Stopwatch, Casio, Japan).

The freezing points were experimentally measured with an instant digital thermometer (P650 series, Serial No.: 65006040472) and a temperature sensor (Pt100, IEC A 240119-1), while the refrigeration system consisted of the following equipment; (a) thermostatic bath (Haake C, Type: 001-0505, Nr: 840096), (b) PID temperature controller (Haake PG 40, Type: 000-9030, Nr: 830264), (c) bath circulator (Haake F3, Type: 000-9601, Nr: 840117), and HTM, which is a mixture of ethylene glycol and deionised water. On the other hand, a DR 5000 Spectrophotometer (Hach, DR 5000, USA) was used to detect the major components (ionic composition) of the feed sample.

2.5. Experimental set-up

Figs. 5 and 6 show the laboratory-scale setup and Sulzer SFC pilot unit, which were used in this investigation. Sulzer have previously designed and constructed this equipment for investigating new fields of application. In this study, the majority of the experiments were conducted with the laboratory setup with the feed materials as mentioned. The pilot plant (Fig. 6), on the other hand, was investigated for concentrating RO brine only.

As shown in Fig. 5a, the laboratory-scale setup consisted of two crystallisers with capacities of 1.5 and 6 L. The two crystallisers each contain a single insulated thermo-stated double wall reaction vessel. These crystallisers were separated from each other, and individually connected to the same refrigeration unit, as shown in Fig. 5b. The internal diameters of these two crystallisers are 50 and 70 mm, respectively, while their lengths are 0.8 and 1.6 m, respectively. These contain a vertical tube, in which the crystal layer grows as a cylindrical shell during the crystallisation operation as shown in Fig. 5c. The crystallisers are made of stainless steel, and each was provided with a stainless steel mesh as shown in Fig. 5d. The mesh was placed underneath the crystalliser (above the sampling valve) in order to avoid the escape of ice crystals during the separation of residual liquid (during draining phase) and sweating fractions (during sweating phase). The feed and sampling processes are shown in Figs. 5e and f.

Fig. 6 shows a schematic diagram of the laboratory-scale setup along with the main equipment. A mixture of ethylene glycol and deionised water was used as a HTM in the refrigeration system. The operating temperature of the HTM was measured via a built-in instant read digital thermometer on the HTM bath circulator. The drain valve (11), which will be known as the sampling point, is a hand-operated stainless steel ball valve installed beneath the crystalliser (Figs. 5f and 6). The underlying purpose is to use this valve to remove (or collect) the water samples (such as residue, sweat fractions, and product) from the crystalliser. As shown in Figs. 5f and 6, the experimental setup was provided with a heat gun pointed towards the sampling valve in order to avoid ice encasing.

Alongside the laboratory-scale setup, a preliminary experimental investigation was carried out on the pilot plant, which has a crystalliser with a capacity of 70 L. Fig. 7a shows the skid mounted pilot plant unit and main equipment used in this investigation. The pilot plant represents a straightforward scale-up pilot unit since the commercial scale crystallizer is designed directly by increasing the surface area and the number of plates in the heat exchanger. In addition, the pilot plant was provided with a heat transfer unit (Huber, Unistat 615) via tubes for low-temperature applications, as shown in Fig. 7b. The heat transfer unit contains a refrigerated thermostatic bath, bath circulator, HTM (Huber, Thermal Fluid: DW-Therm M90.200.02), and PID temperature controller. The crystalliser of the pilot plant was provided with three vertical heat exchanger plates, in which four crystal layers grow

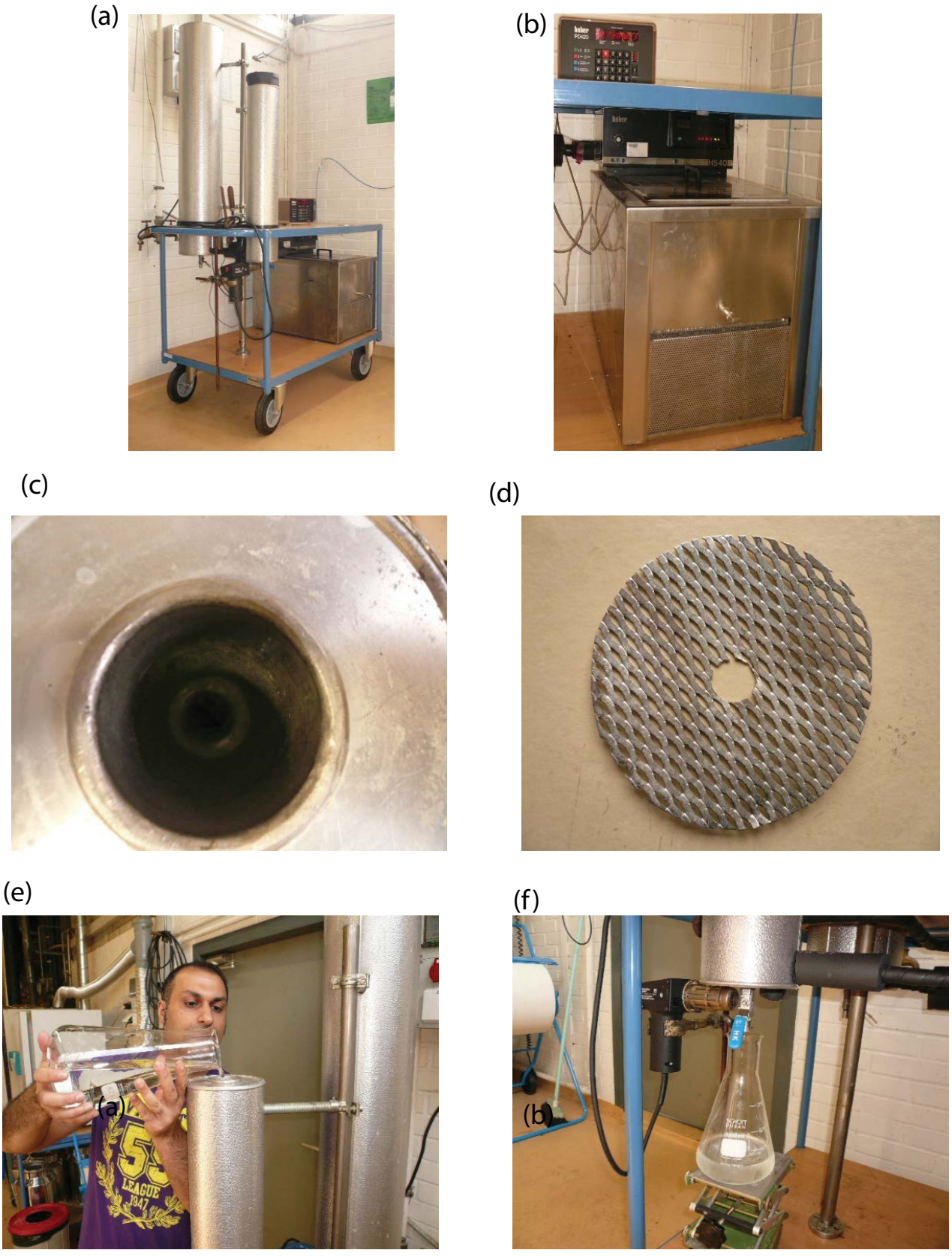

Fig. 5. Laboratory pilot-scale setup and main equipment and processes. (a) Experimental setup, (b) refrigeration system, (c) top view of a crystalliser with ice layer, (d) stainless steel mesh, (e) feeding process, and (f) sampling process.

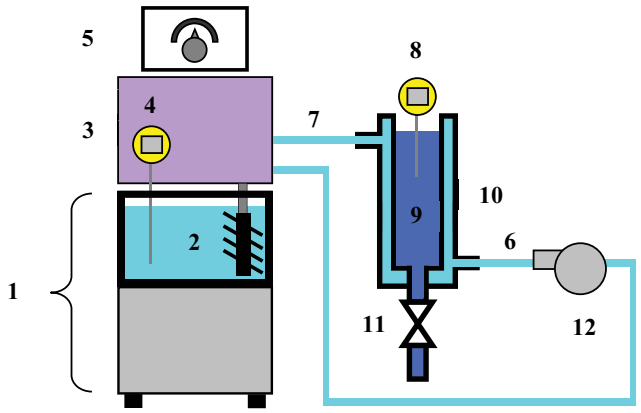

Fig. 6. Schematic of laboratory pilot-scale setup with (1) refrigeration unit and thermostatic bath (Huber, HS 40, Renggli Laboratory Systems Germany); (2) heat transfer medium (HTM); (3) HTM bath circulator (Huber HS 40); (4) built-in digital thermometer; (5) PID temperature controller (Huber PD 420); (6) and (7) inlet and outlet HTM pipelines, respectively; (8) instant digital thermometer (Taylor , USA, Model: 9847N); (9) feed sample; (10) double-wall reaction vessel; (11) sampling valve (HK, stainless steel ball valve, O.D 1/4″); and (12) heat gun (Weller 1095).

as ice slabs during the crystallisation operation as shown in Figs. 7c and d. The height and width of this crystalliser tank is 2 m × 0.5 m, whereas each vertical heat exchanger plate is 1.95 m × 0.45 m. The pilot plant was provided with a laboratory balance (Mettler-Toledo GmbH, ID1 Plus, USA) attached to the crystalliser's tank in order to measure the loaded mass of feed material inside the crystalliser. Also, the pilot plant was provided with a removable stainless steel funnel for the purpose of facilitating the filling process (Fig. 7e) and a drain valve (Fig. 7f).

In general, the concept of the refrigeration systems used for the two laboratory setups is the same. The refrigeration system involves the use of a PID temperature controller and refrigeration unit, attached to the thermostatic bath. The thermostatic bath stores HTM. The refrigeration system has a HTM pump, which is connected to the crystalliser by means of inlet and outlet insulated metal hoses. The HTM pump circulates the HTM from the thermostatic bath into the crystalliser. The process set-point temperature and time are controlled by means of the PID temperature controller.

2.6. Experimental procedure

The principal unit operations considered in the crystallisation experiments were pre-cooling, seeding, crystallisation, residue separation, total melting, and product separation. For the sweating experiments, a partial melting process was considered with the mentioned principal unit operations. The operating procedures for crystallisation and sweating operations using both experimental setups are shown in Fig. 8.

The experiments were investigated in batch mode. Prior to conducting any test, the feed sample was prepared and then the physiochemical analyses were performed. During this process, the refrigeration system was operated, and simultaneously the internal circulation of the HTM took place inside the crystalliser. As illustrated in Fig. 3, the investigated set-point temperatures and running times were set at desired values on the PID temperature controller without activation of the refrigeration operational cycle. The reason behind this is to give enough time for the refrigeration system to cool down, and be prepared for the test, before starting the experiment. Then the sampling valve was fully closed, and the crystalliser was filled with the desired mass of feed sample (Fig. 5e for an example). The crystalliser was then covered with a lid (Fig. 5a). The purpose of using a rubber lid is to protect the feed material from the entry of undesirable materials, such as dust, suspended matter, particles, etc.

The operational cycle of the refrigeration system was turned on, leading to the predetermined set-point temperatures and times that were inserted into the PID temperature controller to be followed (Fig. 3). At the initial stage, the crystalliser was refrigerated by internal circulation of the HTM. Therefore, when the feed temperature reaches a value slightly lower than the freezing point, which represents the start-point temperature for crystallisation (see t_1 in Fig. 3), because of the heat transfer resistance, a seed ice crystal was added to the crystalliser to achieve formation of ice crystals, which were then gradually grown as a cylindrical shell (for the case of the laboratory-scale setup) or an ice slab (for the case of the pilot plant) on a cooled surface immersed in the feed over the duration of the experiment. This crystal layer was progressively and slowly grown on a refrigerated surface perpendicularly outward to the surface leading to the formation of an evenly thin crystal coat on the refrigerated surface.

When the HTM temperature reached the end-point temperature of crystallisation (see t_2 in Fig. 3), the sampling valve at the bottom of the crystalliser was opened manually to collect the remaining liquid phase (i.e., residue) in a laboratory beaker (for the case of the laboratory-scale setup) or a stainless steel barrel (for the case of the pilot plant). The ice layer remained adhered to the refrigerated surface until the end of the draining stage (see t_3 in Fig. 3).

When the temperature of the HTM reached the start-point temperature for partial melting (i.e., sweating), the collection vessel was replaced with another vessel to collect the sweated melt, while the vessel which contained the residue sample was taken for physiochemical analysis. For the sweating experiments, the crystal layer was further purified by conducting a partial melting process (see t_3 and t_4 in Fig. 3). This was achieved practically by gently increasing the temperature of HTM to a desired temperature, leading to gradual heating of the crystal layer inside the crystalliser. Hence the ice crystal layer partially melted inside the crystalliser as the temperature of the HTM increased. According to the predetermined mass of sweated melt and time, this sweated melt, including trapped and adherent material, was collected throughout the sweating operation. This means that the sampling valve was set to fully open until the end of the sweating process. According to Ulrich and Glade [18], the partial melting process is similar to a washing process used in a suspension crystallisation technology, and serves as further purification of the adherent crystal layer. All beakers including the sweated melts were then taken for further analyses. For crystallisation experiments, the process set-point temperature and

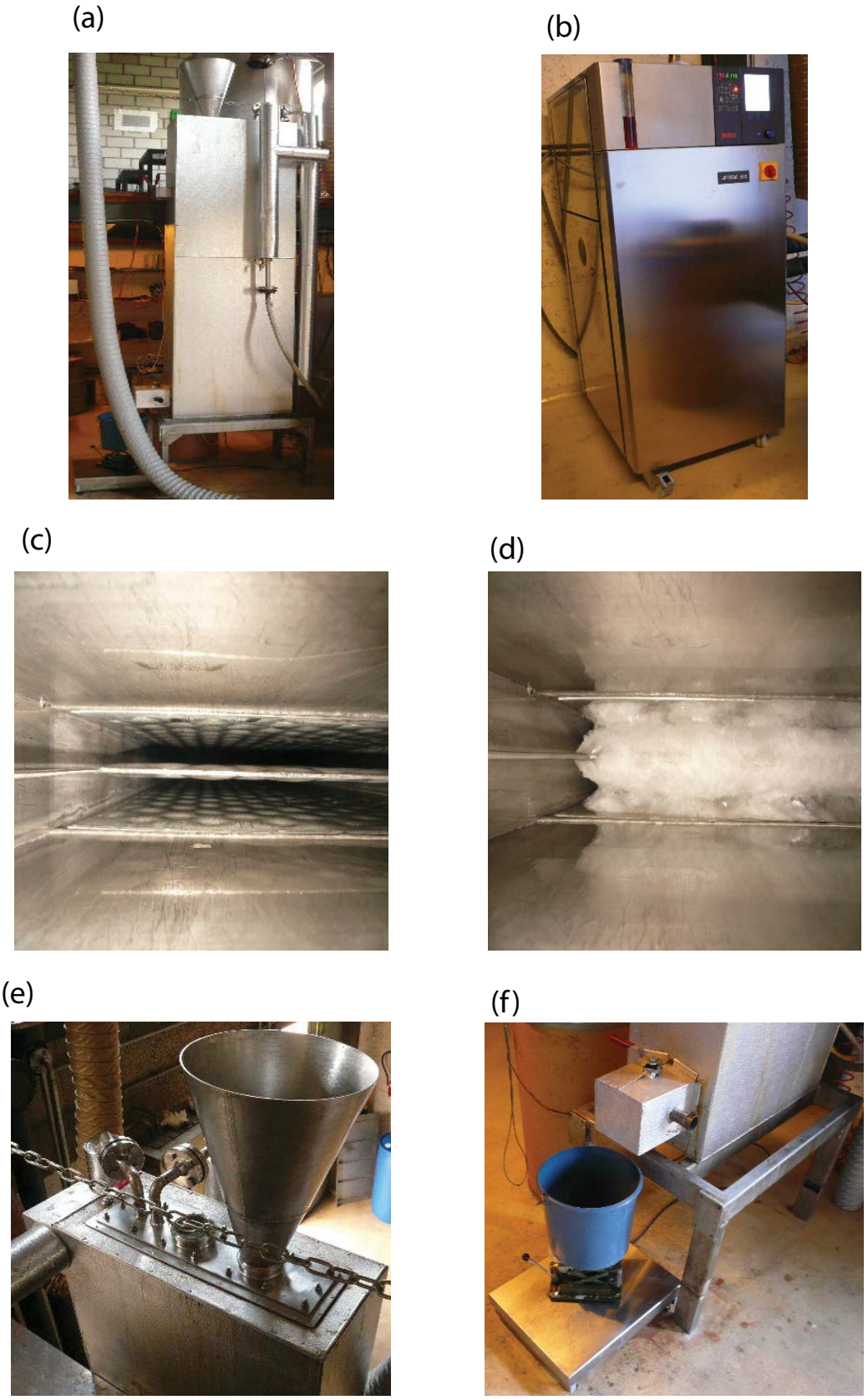

Fig. 7. Pilot-plant apparatus and main equipment. (a) Pilot plant crystallizer, (b) refrigeration unit, (c) internal view of an empty crystallizer, (d) a crystalliser with crystal layer, (e) funnel and top-view of crystallizer, and (f) drain valve (sampling point).

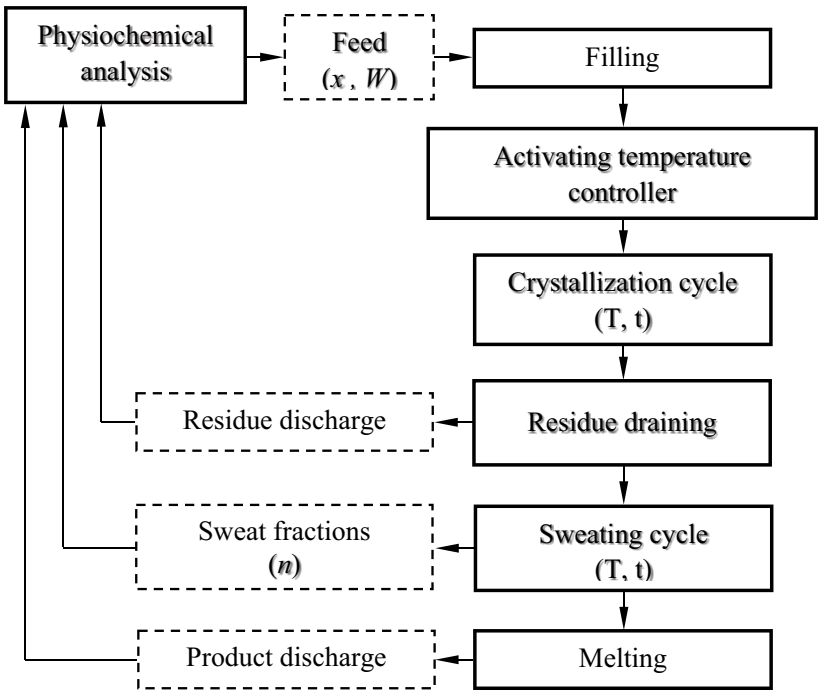

Fig. 8. Simplified block diagram of the operational process for the experiments, where x_f is the feed concentration (ppm), W is the sample weight (kg), t is the running time (minute), T is the temperature (°C), and n is the number of sweat fractions.

time for partial melting operation were set at specific values minimising the running time of the partial melting process, leading to a reduction in the total running time of one crystallisation stage. The sampling valve was set to fully closed, since the sweated melt samples were not collected in the case of the crystallisation experiments.

When the endpoint temperature of the sweating process was reached, for the case of sweating experiments, the vessel which contains the sweated melt was replaced with another vessel for collecting the final water sample, that is, product water. For the crystallisation experiments, the sampling valve at the bottom of the crystalliser was manually opened to collect the melted crystal layer, that is, product water. The melting operation was applied by further increasing the temperature of HTM to the desired temperature at which the remaining/purified crystal layer was totally melted to provide the product water (see t_5 in Fig. 3). The product water was drained off from the crystalliser through the sampling point and taken for further analysis.

3. Results and discussion

Key parameters have been varied and the results have been plotted as a series of graphs. Based on the experimental results, empirical polynomial correlations were derived and fitted for the freezing point as a function of TDS value (ppm), salt concentration (wt.%), and electrical conductivity (mS/cm). Furthermore, the empirical polynomial correlations were also derived and fitted for the electrical conductivity (mS/cm) as a function of salt concentration (wt.%). These equations were also used to instantly determine the results of the main key parameters through the conductivity measurement.

Fig. 9a shows the experimental phase diagram, and empirical graph and equation (including R value) for the AG seawater and RO brine. The important observations that can be revealed from the phase diagram are as follows: (i) the freezing points of AG seawater and RO brine were –2.4°C and –3.1°C, respectively, (ii) the eutectic temperature for the AG seawater and RO brine was –20.45°C, which was obtained at TDS value, electrical conductivity, and weight ratio of 238,560 ppm, 220 mS/cm, and 23.85 wt.%, respectively.

For all tests, the results of the average growth rate were analytically computed by assuming that the dimensions and shape of the solid ice layer are for cylindrical geometry, in the cases using a crystalliser tube, and rectangular geometry, for the cases using a plate heat exchanger. The cooling rates were analytically calculated by dividing the temperature difference, between the end-point and start-point temperatures of the crystallisation operation, by the crystallisation time [18]. The theoretical power consumption for the SFC experiments was analytically determined by the heat transfer rates for cooling the feed water and changing the phase of the liquid, as described previously in the literature [25]. The experimental conditions that have been used in this study are shown in Table 3.

3.1. Parametric study of crystallisation and sweating processes

The first group of experiments was carried out with feed samples using aqueous solutions of sodium chloride. These experiments were performed on the laboratory-scale setup using a 1.5 L capacity crystalliser. The investigated salt concentration of the feed samples was 3.5 wt.%. These experiments were performed in a feed stage process, that

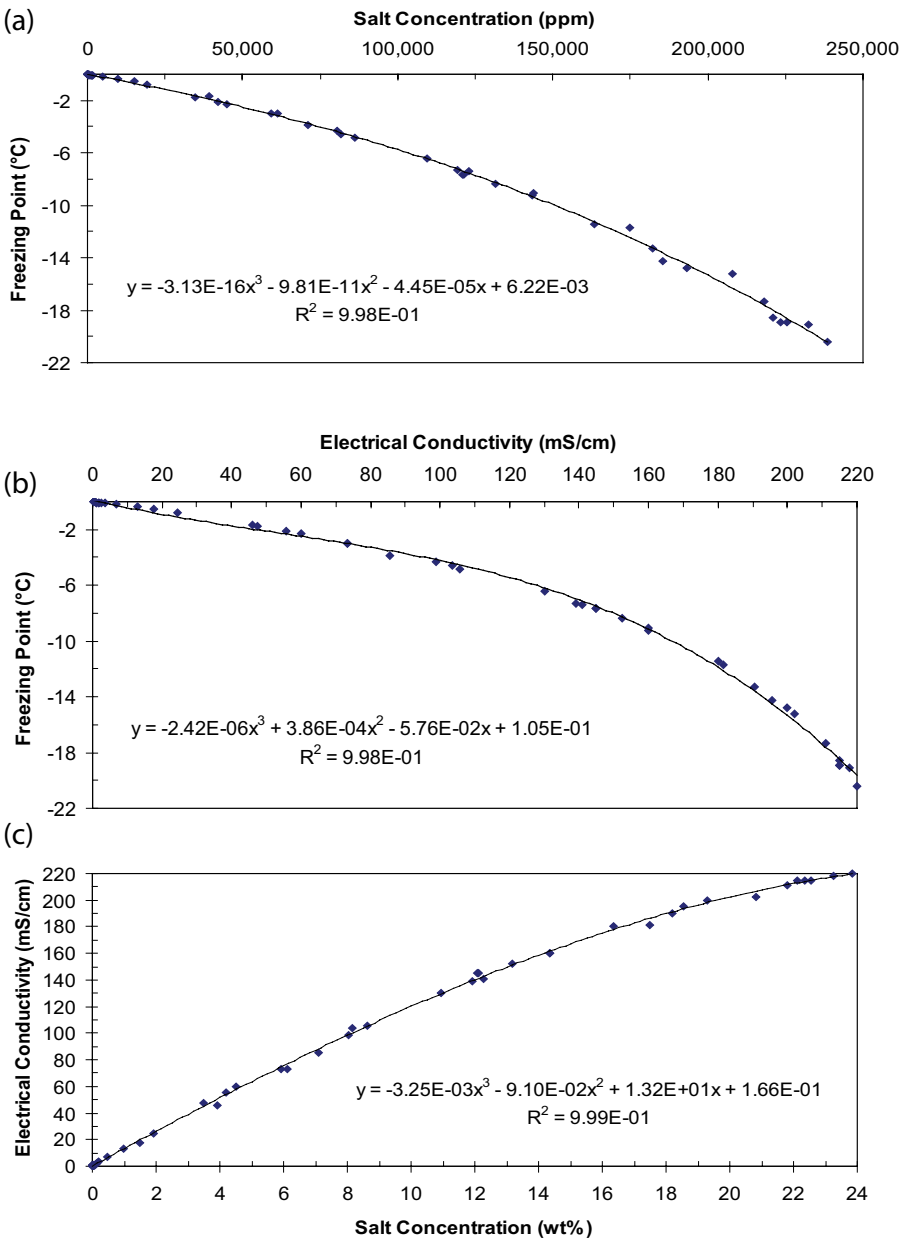

Fig. 9. Summary of the phase diagram and relationships between the main key parameters for the Arabian Gulf seawater and reverse osmosis brine, where y and x are the dependent and the independent variables of the empirical equation, respectively, and R^2 is the polynomial regression correlation coefficient. (a) Phase diagram, (b) conductivity vs. freezing point, and (c) salt concentration vs. conductivity.

Table 3
Operating parameters and conditions for crystallisation and sweating experiments, where PP is the pilot plant and LPS is the laboratory pilot-scale setup

Run No.	Exp. setup	Feed source	Feed conc.	Crystallisation		Sweating	
				Time	End-point HTM temp.	Time	End-point HTM temp.
			(%)	(h)	(°C)	(h)	(°C)
1–7	LPS	NaCl solution	3.5	2–24	–2.3–8.0	2	–2.9–0.8
1–14	LPS	Process brines	5.1–15.0	3.5–12.5	–10– –23	1–4	–23–0
1–8	PP	RO brine	6.1	4–24	–4	–	–

is, single freezing stage. The operating conditions tested are illustrated in Table 4.

A summary of the experimental data for runs 1–3 (i.e., crystallisation experiments) is given in Table 5. The salt rejection ratio was found to be inversely proportional to the average growth rate. However, the water recovery ratio was found to be proportional to the average growth rate (Table 5). For instance, by comparing the results of run 1 and 3, the salt rejection (SR) increased from 24.2% to 59.0% when the average growth rate was reduced from 5.63 to 0.04 mm/h. The water recovery (WR) was significantly reduced from about 70.0% to 8.3%. The salt concentration of product water, on the other hand, decreased (i.e., improved) as the end-point temperature of the crystallisation operation reduced, as illustrated in Table 5. This indicates that the product quality is sensitive to the variations of the end-point temperature of crystallisation operation.

As illustrated in Table 4, the apparatus was also examined for different time retention of the crystallisation operation, ranging from 12 to 72 h (see runs 4 – 7). These experiments were carried out at constant operating conditions for the sweating process. The salt concentrations of crystal layers, before and after the sweating process, were investigated. A summary of the experimental results is given in Fig. 10. The figure (Fig. 10a) shows that the salt rejection ratio was dramatically reduced after increasing the average growth rate. This confirms the previous findings regarding the influence of the average growth rate on salt rejection ratios, as well as the effect of sweating [6]. Fig. 10b shows the salt rejection ratio as a function of the cooling rate of the crystallisation process, as well as the effect of sweating. The results show that the lower growth rates, dictated by slow crystallisation rate (i.e., higher cooling rates), are of great importance in improving the separation performance of the static crystallisation process. These findings are compatible with previous work [6] on the effect of cooling rate and average growth rate on the salt concentration of the product water. The effect of crystallisation time on the salt concentration of product can be observed in Fig. 10c, when the end-point temperature was maintained at a constant value. The results indicate that the process is very sensitive to changes in crystallisation time. By comparing the purity of crystal layers, before and after the sweating process, the salt rejection ratio was improved by using the sweating process, as shown in Fig. 10c. A strong decrease in salinity of the crystal layer was observed when the sweating process was applied. Furthermore, the total freezing stage time was dramatically reduced, when compared with that in the crystallisation operation without sweating. For instance, a crystal layer was obtained at a salt concentration of 0.73 wt.% by using the crystallisation process separately (i.e., without sweating process) with a crystallisation time of 72 h; in contrast, another crystal layer was produced at a lower salt concentration (i.e., 0.44 wt.%) and

Table 4
Operating conditions of crystallisation and sweating tests using 1.5 L static crystalliser for treating NaCl solutions

Run	Feed			Crystallisation			Sweating		
	M	C	FP	T_1	T_2	t_C	T_1	T_2	t_S
	(g)	(wt.%)	(°C)	(°C)	(°C)	(h)	(°C)	(°C)	(h)
1	1,500	3.5	–2.2	–2.30	–8.00	2	Not applied		
2					–6.00				
3					–2.90	24			
4						12			
5						24			
6						36	–2.90	0.80	2
7						72			

The notations such as M, C, and FP represent mass, salt concentration, and freezing point, respectively, whereas T_1 and T_2 represent the start-point and end-point temperatures, respectively, while t_C and t_S represent running times of crystallisation and sweating processes, respectively.

Table 5
Experimental data of crystallisation tests using runs 1–3

Run	Feed			AGR	Product			WR	SR	Residue		
	M	C	FP		M	C	FP			M	C	FP
	(g)	(%)	(°C)	(mm/h)	(g)	(%)	(°C)	(%)	(%)	(g)	(%)	(°C)
1	1,500	3.5	–2.2	5.63	1,048	2.7	–1.7	69.9	24.2	452	5.5	–3.5
2	1,500	3.5	–2.2	3.96	801	2.4	–1.5	53.4	31.3	699	4.8	–3.0
3	1,500	3.5	–2.2	0.04	124	1.4	–0.9	8.3	59.0	1,376	3.7	–2.3

The notations are as follows: M, C, and FP represent mass, salt concentration, and freezing point, respectively; AGR, WR, and SR represent the average growth rate, permeate water recovery, and salt rejection, respectively.

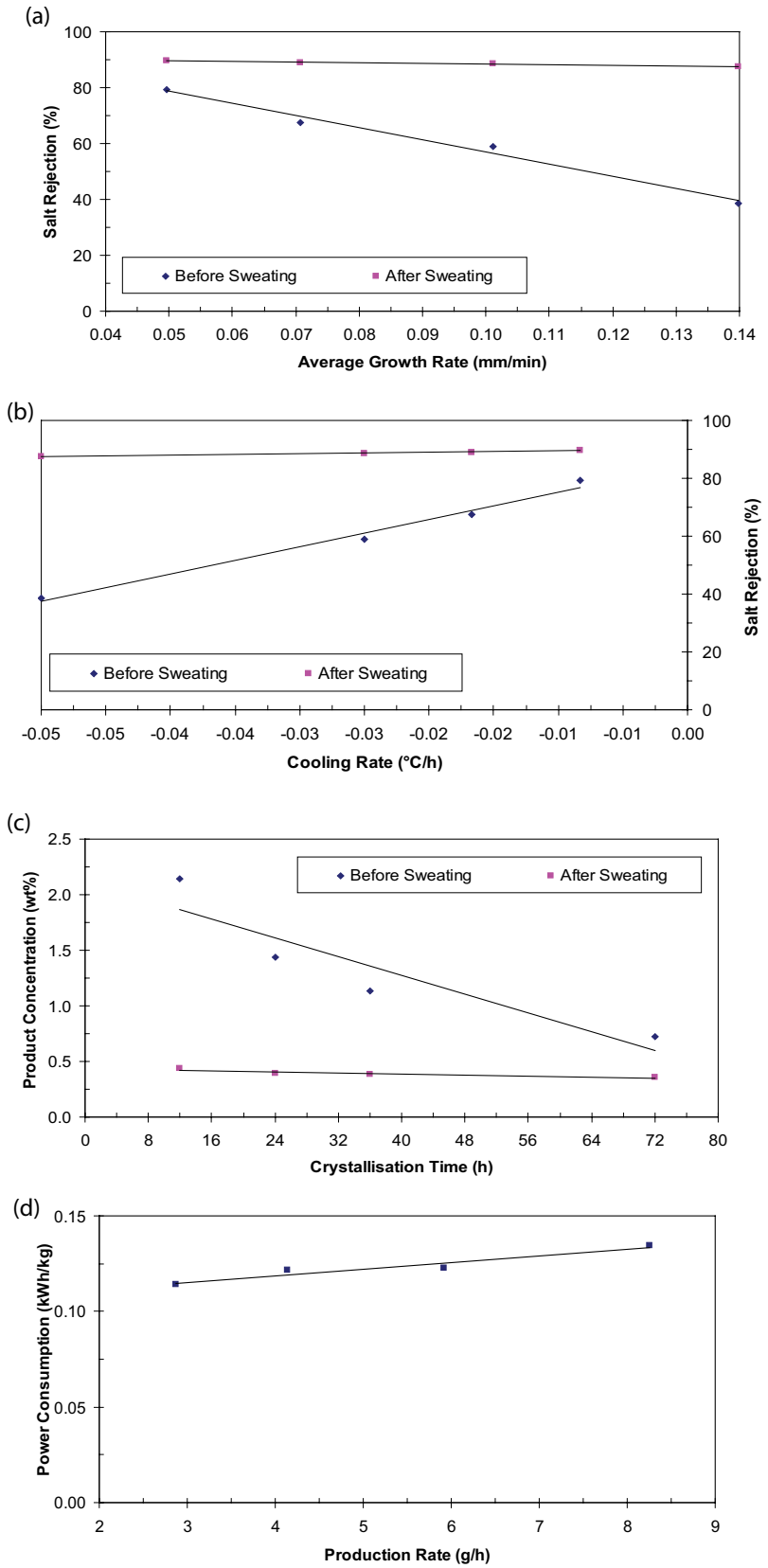

Fig. 10. Preliminary experimental results for the static crystallisation and sweating experiments using the operating conditions of runs 4–7. (a) Salt rejection ratios vs. growth rate, (b) salt rejection vs. cooling rate, (c) product concentration vs. crystallisation time, and (d) power consumption vs. production rate.

at lower crystallisation time (i.e., 12 h), when a sweating operation was incorporated into the static crystallisation process, and applied for 2 h. Therefore, the experimental results suggested that it would be an ideal treatment system to optimise the operating conditions of crystallisation and sweating operations to achieve the desired quality rather than optimising and applying the crystallisation operation separately. The calculations of theoretical power consumption for the experiments, on the other hand, give an average value of 0.123 kWh/kg as shown in Fig. 10d.

3.2. RO brine treatment – using a pilot plant with a crystalliser capacity of 70 L

In the second series of experiments, the potential capability of the Sulzer SFC process pilot plant (without use of a sweating process) for concentrating and treating RO brine was investigated. These experiments were carried out using a feed-stage process.

The investigated volume of feed water was 70 L. The actual operating period of the crystallisation experiments was varied from 4 to 24 h. The investigated start-point and end-point temperatures of crystallisation operation were –4°C and –8°C, respectively. The results of the separation performance and the computed power consumption of the investigated pilot plant are shown in Fig. 11. Results of salt concentration of product, as a function of the growth and cooling rates are shown in Figs. 11a and b, respectively. The trends of these results are clearly observed to be in agreement with the first series of the experiments. As shown in Fig. 11c, the minimum and maximum salt concentrations of product water were 3.46 and 4.49 wt.%, respectively, and the water recovery stabilised at an average value of 73%. This indicates that the investigated pilot plant, within the study domain, was capable of providing a substantial amount of product water of near ocean seawater standards. As a result, the treated water can be further easily desalted either by a sweating process, increasing the number of rectification stages, or simply by recycling the treated water into the main feed stream of a seawater RO membrane plant to obtain a final product of drinking water. When the desired salt concentration of product water is required to be similar to that of Arabian Gulf seawater, then the experimental results suggested reducing the retention time of the crystallisation process (i.e., less than 4 h). This is because crystal layers were experimentally produced at a lower salt concentration, when compared with Arabian Gulf seawater. By reducing the overall running time of the freezing stage, a significant increase in the production rate would be expected, which will lead to a dramatic fall in the operational cost. As for the energy consumption, Fig. 11d shows a plot of the theoretical results of the power consumption vs. the production rate. The theoretical power consumption for the investigated pilot plant gave an average value of 97 kWh/m^3.

3.3. Process brine treatment – using the laboratory pilot-scale setup with a crystalliser capacity of 6 L

The third group of experiments were carried out on feed samples using process brines to determine the number of influences on the performance of the SFC process. These experiments were carried out on the laboratory-scale setup using a crystalliser capacity of 6 L. The experiments were performed in a feed-stage process, using crystallisation and sweating processes. The salinities of the crystal layers, before and after the sweating process, were studied.

The first investigation was carried out on feed samples using concentrated RO brine with a salt concentration of 12 wt.%; this was previously taken from the residue sample of suspension crystallisation experiments (details of the previous study are available in the literature [19]). This investigation was carried out to determine the influence of the cooling rate of crystallisation operation on the salt separation of the SFC process as well as the effect of the sweating process. The investigated cooling rates were –0.48 and –0.80°C/min, whereas the sweating process was maintained at constant operating conditions.

Figs. 12a and b show the influences of several factors, such as: cooling rate of crystallisation operation, crystal mass ratio, and sweating time, on the salt concentration of the crystal layer. The salt concentration of the crystal layer decreased (i.e., improved) as the cooling rate of the crystallisation process increased, as observed previously in different experiments. For instance, before performing the sweating process, the salt concentration of the crystal layer was reduced from 9.78 to 8.40 wt.% by decreasing the cooling rate of the crystallisation process from –0.80 to –0.48°C/min (Fig. 12a). Figs. 12a and b show that the sweating process was found effective in improving the salinity of the crystal layer, where a notable reduction in the salt concentration of product was observed through increasing the crystal mass ratio and sweating time. For instance, for the case of the crystallisation rate of –0.80°C/min, the salt concentration of the crystal layer was reduced from 9.78 to 4.50 wt.% when the crystal mass ratio reached 35.64%.

For the case of the crystallisation rate of –0.48°C/min, the salinity of the crystal layer was further reduced by the sweating process, where the salt concentration of the crystal layer was lowered from 8.40 to 3.68 wt.% when the crystal mass ratio reached 36.25%. In general, the salt rejection ratio was increased, via a sweating operation, as the crystal mass ratio and sweating time increased. For instance, in the case of a crystallisation rate of –0.48°C/min, the salt rejection ratio before the sweating process was 29.96%. In contrast, the final salt rejection ratio increased to 67.84% after performing the sweating operation under the investigated operating conditions. The trend of this finding was also in agreement with the case of the crystallisation rate of –0.80°C/min, where the salt rejection ratio, before a sweating operation, was 18.50%. The final salt rejection ratio, in contrast, was increased to 62.46% after carrying out the sweating process.

When the desired salinity of the crystal layer is required to be near that of Arabian Gulf seawater, then the experimental results suggested reducing the time retention in the crystallisation process to 3 and 2 h for the cases of the crystallisation rate of –0.80 and –0.48°C/min, respectively. In contrast, when the desired salinity of the crystal layer is required to be near the RO brine (6.11 wt.%), then the experimental results suggested further reduction in the time retention of the crystallisation process to 2 and 1 h for the crystallisation rates of –0.80 and –0.48°C/min, respectively.

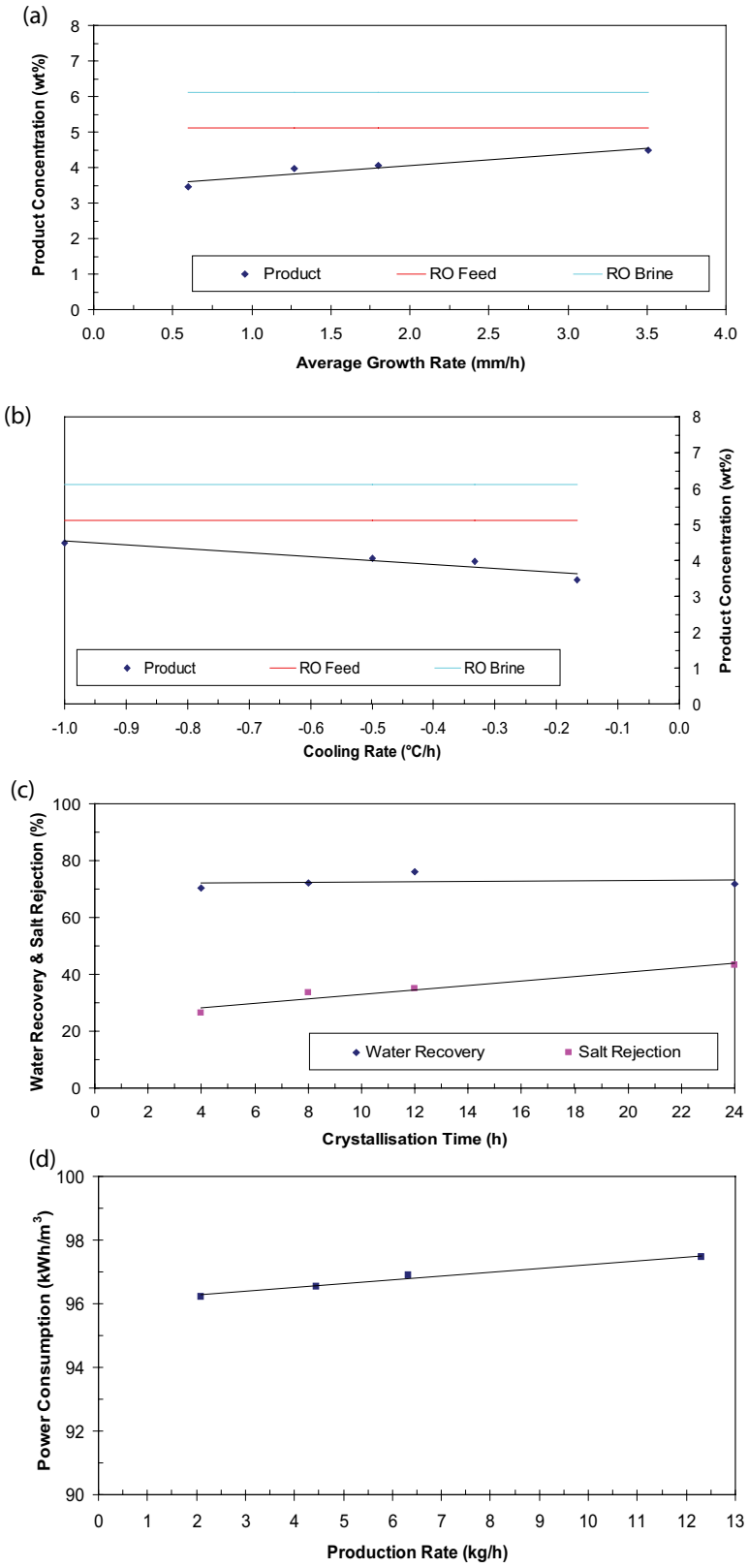

Fig. 11. Summary of experimental results for the static crystallisation pilot plant used for treating RO brine. (a) Production concentration vs. growth rate, (b) production concentration vs. cooling rate, (c) water recovery and salt rejection vs. crystallisation time, and (d) power consumption vs. production rate.

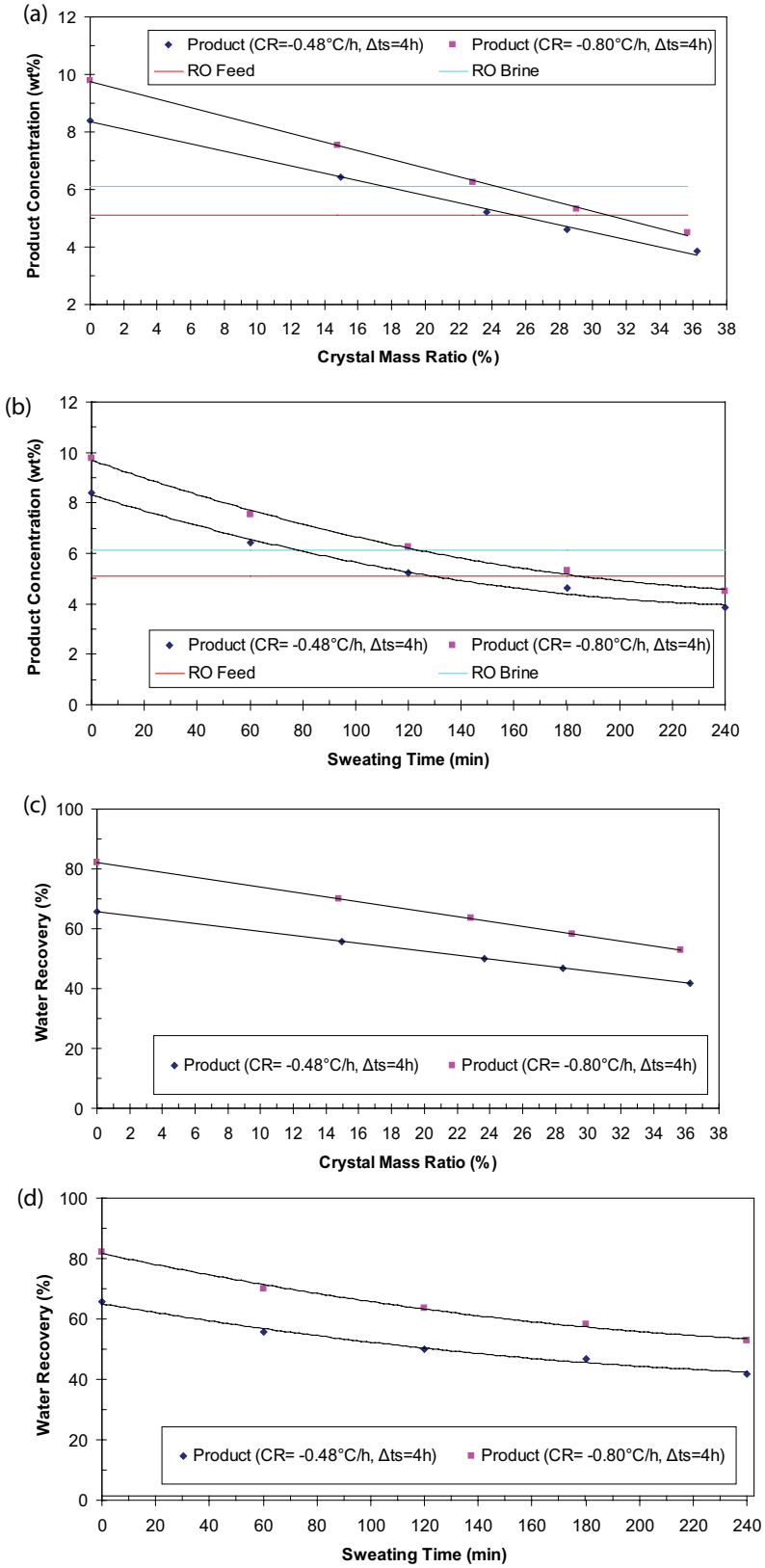

Fig. 12. Influence of cooling rate of the crystallisation process and effect of the sweating process on the salt concentration of the crystal layer and permeate water recovery ratio, where CR is the cooling rate, and Δt_s is the sweating time. The investigated feed water concentration was 12 wt.%, using the concentrated RO brine disposed from the suspension crystallisation experiments (see literature [19]). (a) Product concentration vs. crystal mass ratio, (b) Product concentration vs. sweating time, (c) Water recovery vs. crystal mass ratio, and (d) Water recovery vs. sweating time.

As mentioned previously, the production rate can be substantially increased by reducing the overall running time of the freezing stage, and thus the operational cost will be dramatically decreased. The results of water recovery ratio and cooling rate of the crystallisation process as a function of the mass crystal ratio and sweating time are shown in Figs. 12c and d. The water recovery was found to decrease with increasing crystal mass ratio and sweating time, and to increase with decreasing crystallisation rate.

The second study was performed using the previous experimental conditions, except for changing the investigated crystallisation rate and sweating time. The examined crystallisation rate was set at constant value, that is, –2°C/min, while the sweating process was carried out at sweating rates of 5.5 and 22.0°C/min. This study was performed to evaluate the change of sweating time on the salinity of the crystal layer. A summary of the experimental results is shown in Fig. 13. Figs. 13a and b show that the salt concentration of the product water was improved as the sweating time was increased. Fig. 13b shows that the salt concentration of the crystal layer was lowered from 11.28 to 8.10 wt.%, when the sweating rate was set to 22°C/min, which corresponds to a poor sweating efficiency. This was because the salt concentration of the final product water was relatively poor when compared with the RO brine. When the sweating rate was set to 5.5°C/min, the salt concentration of crystal layer decreased to 4.74 wt.%, which corresponds to a reasonable separation performance since the final product water is close to Arabian Gulf seawater standards. In other words, the salt rejection ratio was significantly increased, via a sweating operation, as the sweating rate increased. For instance, the calculations of the salt rejection ratio, before the sweating operation, give 4.38%, while the final salt rejection ratio, in contrast, was increased to 32.47% after carrying out the sweating process at a sweating rate of 22°C/min. In contrast, the salt rejection ratio was significantly increased to 60.47% after performing the sweating operation at a sweating rate of 5.5°C/min. This clearly indicates that the salt rejection ratio is inversely proportional to the sweating rate.

When the desired salt concentration of the crystal layer was required to be close to that of the RO brine, then the experimental results suggested lowering the sweating time down to 3 h for the cases of the sweating time 5.5°C/min; in contrast, the sweating time must be further extended for the sweating rate of 22°C/min to reduce the salt concentration of crystal layer down to that of the RO brine. However, this action may be accompanied by a dramatic fall in the water recovery ratio, when compared with that in the sweating process with lower rates. As previously mentioned, the reduction in the sweating time has a positive impact on the production rate and operational cost. The crystal mass ratio was found to be proportional to the sweating time, as shown in Fig. 13c. The water recovery ratio was dramatically decreased as the sweating time is increased (Figs. 13c and d).

The third investigation was performed with two different types of feed samples using Arabian Gulf seawater and RO brine. This investigation was performed to find out the effect of feed salt concentration on the quality of the crystal layer at low crystallisation temperature. The investigated end-point temperature of crystallisation was set at –23°C, which was slightly lower than the eutectic temperature of NaCl. The crystallisation and sweating times were set at 5.5 and 4.0 h, respectively. The experimental results of the investigated treatment system are shown in Fig. 14.

The experimental results clearly indicate that the separation performance of the crystallisation and sweating processes were negatively affected by a slight increase of the salt concentration of the feed water, as shown in Figs. 14a and b. The product concentration was found to be proportional to the feed concentration, in agreement with all previous experiments. However, the water recovery ratio did not change with a slight increase in the salinity of feed water. As shown in Figs. 14c and d, the amount of residue samples was nil, which was due to the amount of feed samples that were completely frozen after carrying out the crystallisation process. Figs. 14a and b show that the sweating process was capable of reducing the salinity of the crystal layer down to 2.49 and 3.64 wt.% for the cases of treating Arabian Gulf seawater and RO brine, respectively.

For the experiment with RO brine, clear signs of solid salts precipitation in the sweat fraction were visually observed. The harvested salts were collected and experimentally measured, giving about 12 g. Table 6 demonstrates the water chemistry results for the water samples. The mass and salt balance calculations showed that the percentage loss in the residual liquid is about 9%. Table 6 also confirms the signs of precipitation of salts composed of Na^+, Cl^-, Ca^{2+}, Mg^{2+}, and $(SO_4)^{2-}$ ions, since the calculations of the percentage losses in their ionic concentration give about 14%, 14%, 26%, 37%, and 20% respectively. The main reason for the solid salts precipitation may be explained by operating the crystallisation process under a critical temperature, which is lower than eutectic temperature of NaCl.

The experimental results suggested, for the case of RO brine concentration, to reduce the crystallisation time from 4 to 1 h to provide a final product water of near the quality of Arabian Gulf seawater, in terms of salinity (Figs. 14a and b). Thus, this action will substantially increase the water recovery ratio from 80.45% to about 99% (Fig. 14d), taking into account that there will be precipitation of solid salts, discharged with sweating fractions for such an application.

The fourth investigation was carried out on RO brine. The investigated end-point temperatures were –10°C and –23°C, where the crystallisation and sweating times were set at 5.5 and 4.0 h, respectively. This investigation was carried out to determine the influence of end-point crystallisation temperature on the salinity of crystal layer and water recovery ratio.

Fig. 15 shows the variation of the salt concentration of crystal layer and water recovery ratio, as a function of the crystal mass ratio and sweating time. A clear tendency of decreasing salt concentration in the crystal layer with increasing end-point crystallisation temperature can be observed as shown in Figs. 15a and b. For example, for the case with an end-point temperature of –23°C, the calculations of the salt rejection ratio, before the sweating operation, give 0%, because the feed sample was completely frozen. In contrast, the final salt rejection ratio increased dramatically to 40.39% after carrying out the sweating process. The salt rejection ratio, before the sweating operation, was 37.73%, for the case where the end-point temperature was –10°C. The salt rejection ratio increased to 65.17% after

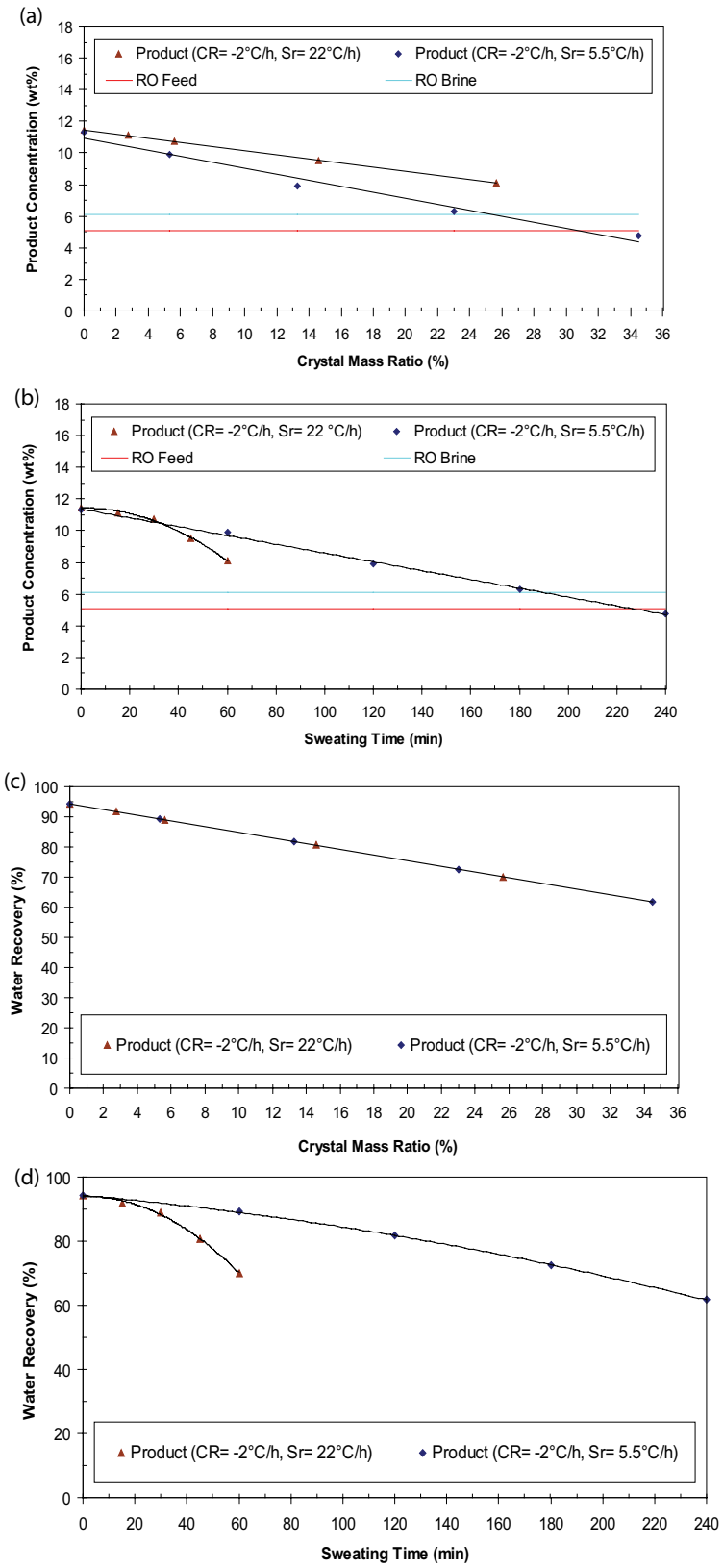

Fig. 13. Influence of sweating time on the salt concentration of the crystal layer and permeate water recovery ratio, where CR is the cooling rate, and Sr is the sweating rate. The investigated feed water concentration was 12 wt.%, using the concentrated RO brine disposed from the suspension crystallisation experiments (see literature [26]). (a) Product concentration vs. crystal mass ratio, (b) product concentration vs. sweating time, (c) water recovery vs. crystal mass ratio, and (d) water recovery vs. sweating time.

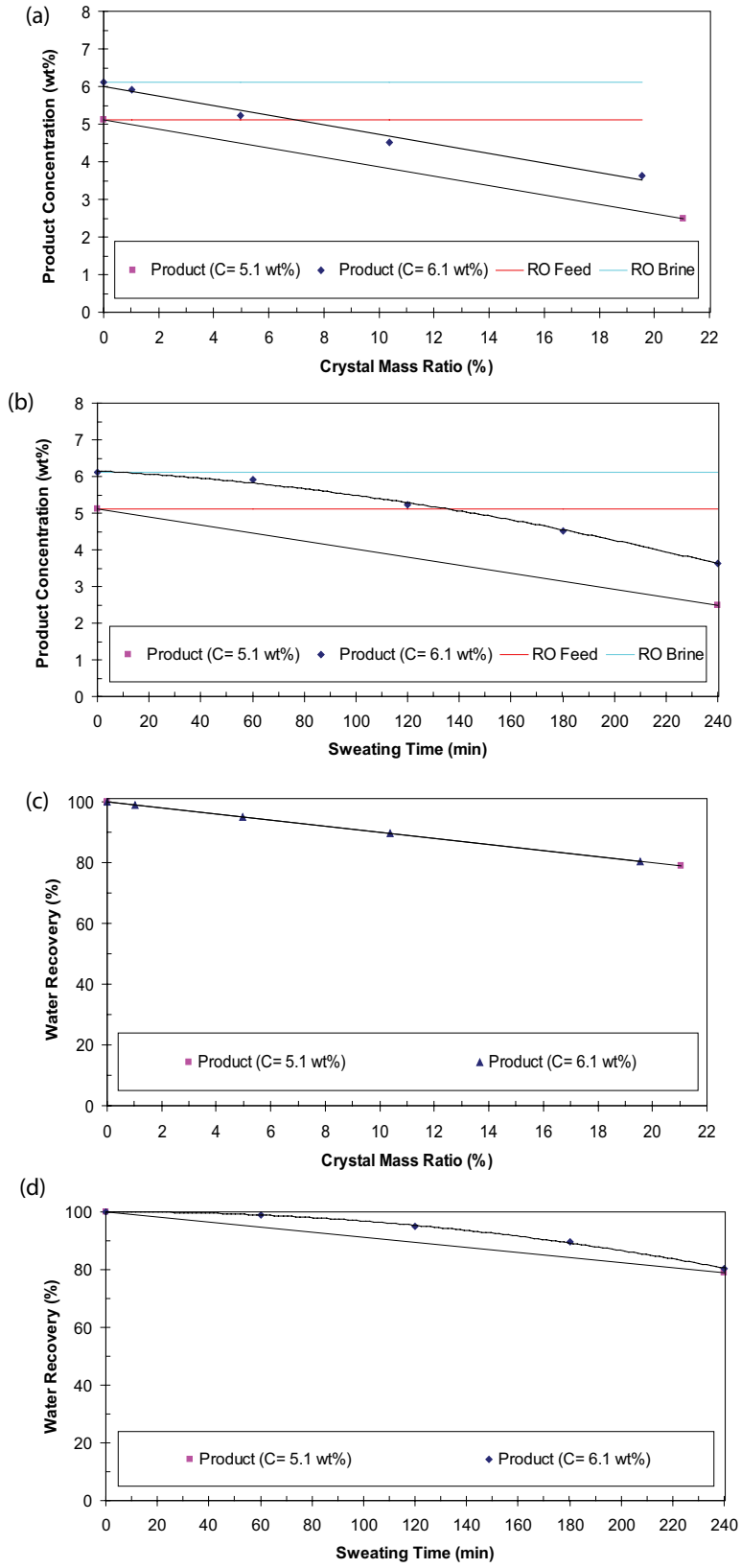

Fig. 14. Influence of salt concentration of feed water on the performance of the static crystallisation and sweating processes, where *C* is the salt concentration of the feed water. The experimental conditions are start-point and end-point temperatures of –5°C and –23°C, respectively, and the sweating time is 4 h. (a) Product concentration vs. crystal mass ratio, (b) product concentration vs. sweating time, (c) water recovery vs. crystal mass ratio, and (d) water recovery vs. sweating time.

sweating. This indicates that the end-point crystallisation temperature is proportional to the salt rejection ratio.

A dramatic increase in the water recovery ratio observed as the end-point crystallisation temperature was reduced as shown in Figs. 15c and d. This gives a clear indication that the water recovery ratio is inversely proportional to the end-point crystallisation temperature. For the test with an end-point temperature of –23°C, the water recovery ratio was 100% (Figs. 15c and d), as the residual liquid was nil during the draining phase, because the mass of feed was completely frozen. As for the performance of the sweating process, the salinity of the final product water reached 2.13 and 3.64 wt.% at end-point crystallisation temperatures of –10°C and –23°C, respectively, whereas the water recovery ratios reached 62.75% and 80.45%, respectively.

In the fifth investigation, the residues discharged from falling film and suspension crystallisation processes were individually collected [19,20], prepared and tested as feed water. This means that the investigation was carried out on two highly concentrated brines with salinities of 14.78 and 13.00 wt.%. The investigated start-point and end-point temperatures were –10°C and –19°C, respectively. The crystallisation and sweating times were set at 5.5 and 4 h, respectively. This investigation was carried out to determine the potential capability of using the SFC technology as a concentration system for concentrating the mentioned residues. The salt concentrations of crystal layers, before and after the sweating process, were measured in order to determine the optimal operating conditions.

Results of salt concentration of product and water recovery, as a function of the crystal mass ratio and sweating time are shown in Fig. 16. Figs. 16a and b show the variation of the salt concentration of the crystal layer (investigated at different feed concentrations) as a function of the mass crystal ratio and sweating time. Agreement with the findings of the previous experiments, concerning the influence of feed concentration, mass ratio, and sweating time, on the product quality is clearly observed. Figs. 16c and d show the effect of several influences, such as feed concentration, crystal mass ratio, and sweating time, on the water recovery ratio. In general, the salinity of the feed waters with salt concentrations of 13.00 and 14.78 wt.% was lowered to 6.11 and 5.06 wt.%, respectively, whereas the final water recovery ratios reached 41.90% and 49.84%, respectively. For the case of a treating feed with a salinity of 13.00 wt.%, the salt rejection ratio, before the sweating operation, was 21.63%, whereas the sweating process was capable of increasing the salt rejection up to 61.10%. In contrast, for the case of treating a feed with a salinity of 14.78 wt.%, the salt rejection ratio, before the sweating operation, was 17.87%, which was then significantly increased to 60.46% after performing the sweating process. The results showed that, for the feed concentration of 14.78 wt.%, the minimum sweating time that should be considered is 4 h. This is because when the sweating time was less than 4 h, relatively poor-quality product water was produced.

As for the feed concentration of 13.00 wt.%, the minimum sweating time that can be considered was either 3 or 4 h. This is because the sweating process at a running time of 3 h was capable of providing a crystal layer of near RO brine standards (Fig. 16a), whereas a sweating time of 4 h can further reduce the salinity of crystal layer, leading to a final product water of near Arabian Gulf seawater, in terms of salt concentration. Thus, production rate will be increased for such an application, leading to a reduction in the operational cost.

Table 6
Water chemistry analysis for concentrating RO brine, where the collected sweating fraction samples were mixed together and identified as "residue*" for the full chemical analysis

Parameter	Feed	Product	Residue*
Mass, kg	6.047	4.865	1.182
Conductivity, mS/cm	76.60	44.60	164.80
Salt concentration, wt.%	6.11	3.64	14.75
Melting point, °C	–3.24	–2.07	–9.62
Ca^{2+}, mg/L	1,476	840	3,040
Mg^{2+}, mg/L	1,463	778	2,717
Na^{+}, mg/L	20,881	15,174	38,324
SO_4^{2-}, mg/L	4,800	3,280	10,790
HCO_3^{-}, mg/L as $CaCO_3$	241.2	161.3	380.7
Cl^{-}, mg/L	32,200	23,400	59,100

4. Conclusions

This experimental study presented a new application for the Sulzer SFC process. The performance of the SFC process was experimentally evaluated and validated for brine concentration applications. Aqueous solutions of sodium chloride and different salinities of process brines were investigated individually as feed samples. The investigation focused on the feed samples of highly concentrated brines, which were discharged from prior processes, namely RO, falling film and suspension crystallisation.

A number of important parameters influencing the separation performance of crystallisation and sweating processes were investigated, not only on the laboratory bench scale but also in a pilot plant (for some experiments). The key findings of the crystallisation experiments provided a clear indication that the investigated parameters, including feed concentration, crystallisation temperature, crystallisation rate, and average growth rate, had a strong influence on the separation performance of the crystallisation step. For example, the salt rejection ratio was found to be proportional to the crystallisation temperature and cooling rate, and inversely proportional to the feed concentration and average growth rate. The water recovery ratio, on the other hand, was found to be inversely proportional to the crystallisation temperature, cooling rate, and feed concentration, but proportional to the average growth rate. As for the sweating process, the separation performance of this technique was found to be strongly dependent on the salinity of the crystal layer, sweating rate, sweating time, and crystal mass ratio. The salt concentration of the crystal layer was found to be inversely proportional to the sweating time and crystal mass ratio, and proportional to the crystal layer salinity and sweating rate. The sweating operation was found to be effective in

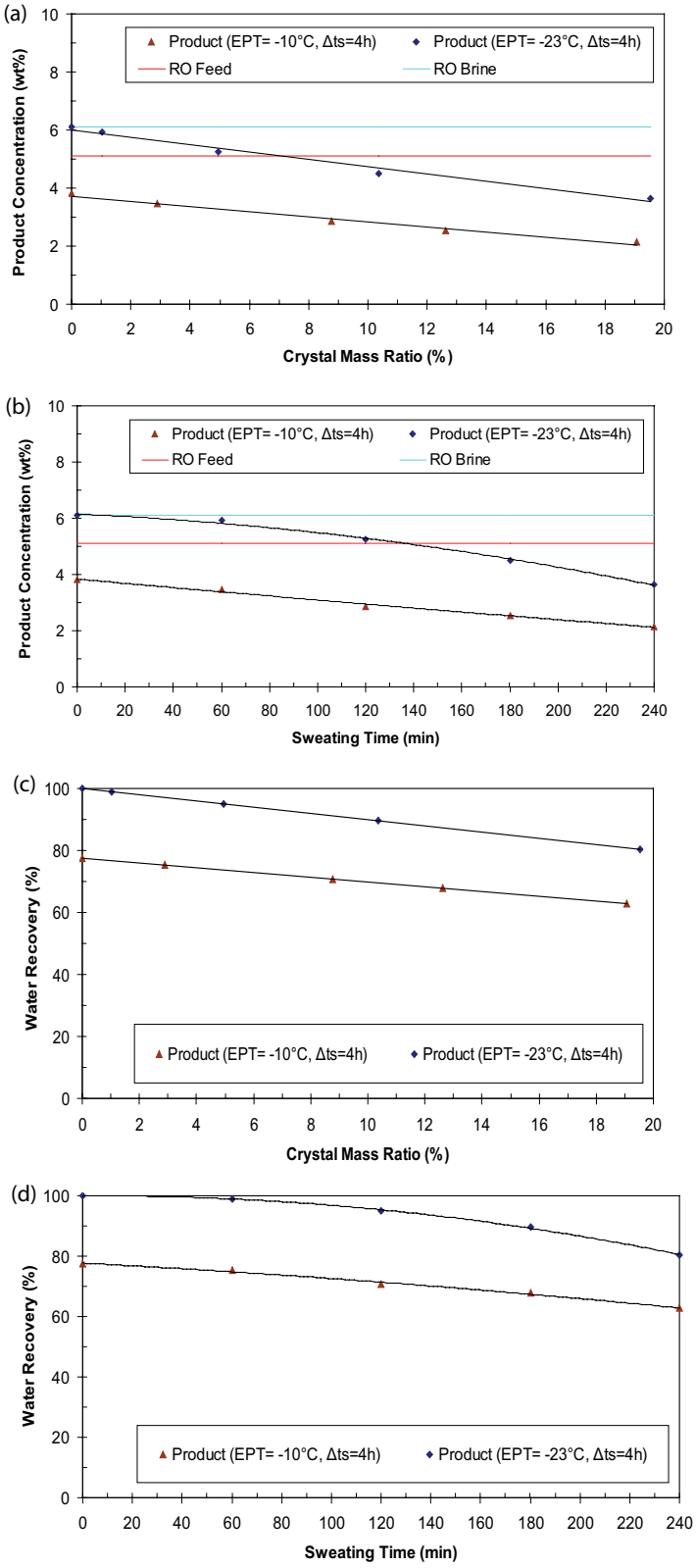

Fig. 15. Influence of end-point temperature of the crystallisation stage on the product water concentration and sweating performance, where EPT is the end-point temperature, and Δt_s is the sweating time. The investigated operating conditions are (i) materials: start and end-point of crystallisation temperature are –5°C to –23°C, respectively, for a crystallisation time of 5.5 h, and (ii) sweating time of 4 h. (a) Product concentration vs. crystal mass ratio, (b) product concentration vs. sweating time, (c) water recovery vs. crystal mass ratio, and (d) water recovery vs. sweating time.

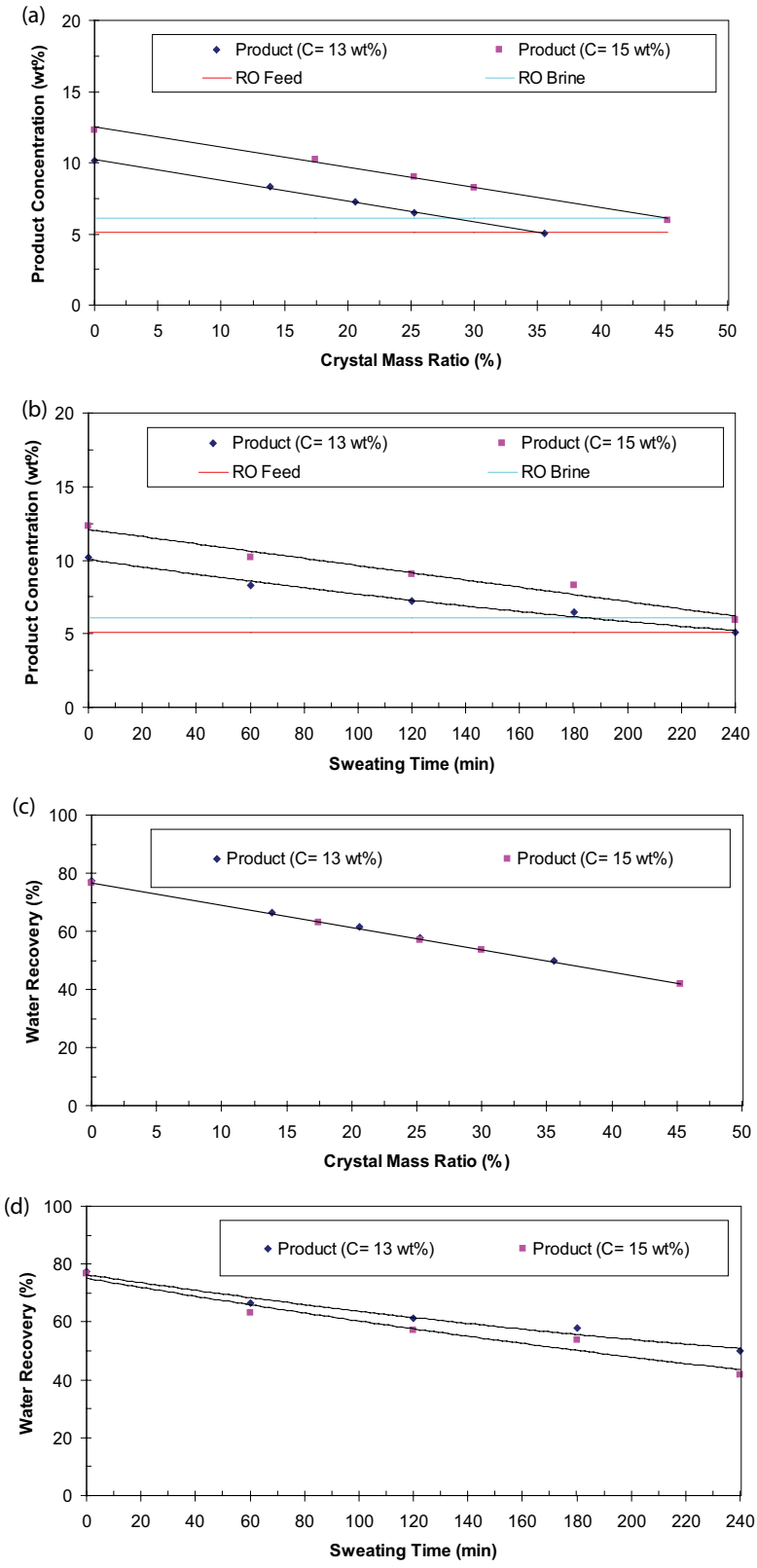

Fig. 16. Operating conditions and experimental results for static crystallisation using laboratory apparatus with a 6 L crystalliser. Operating conditions are feed solutions of RO brine (with concentrations of 13 and 15 wt.%, respectively), start and end point of crystallisation temperature are –9°C to –19°C, respectively, at a crystallisation time of 12.5 h, and sweating time of 4 h. (a) Product concentration vs. crystal mass ratio, (b) product concentration vs. sweating time, (c) water recovery vs. crystal mass ratio, and (d) water recovery vs. sweating time.

improving the purity of the crystal layer, and enhanced the separation efficiency of the SFC process. However, the disadvantage of using the sweating method is associated with two crucial factors, namely mass loss and freezing-stage time. Therefore, the sweating rate must be optimised at a reasonable limit to minimise the mass loss, and reduce the time of the freezing stage; otherwise a substantial increase in the investment costs of water treatment will be encountered. In order to provide final product water at reasonable cost and reasonable reliability, the investigated influences of the crystallisation and sweating operations, more specifically the cooling and sweating rates, must be appropriately co-optimised.

The experimental results for concentrating RO brine, using a pilot plant, proved that a single-freezing stage, without use of the sweating process, was capable of producing a significant amount of treated water, while the RO retentate was concentrated to a reasonable level. The salinity of the treated water was found to be comparable with Arabian Gulf seawater, and was ready for immediate re-use as feed water for an RO membrane desalination plant. By eliminating the sweating process, several advantages can be rendered to the Sulzer SFC plant, for instance, mass loss will be avoided, a dramatic fall in the overall time for the freezing stage, significant increase in production rate, and a noticeable reduction in power consumption.

On the other hand, the RO brine was tested at various crystallisation temperatures, which were higher and lower than the eutectic temperature of NaCl. These experiments were performed on the laboratory pilot-scale setup with use of the sweating process. Similar findings to the earlier experiments were observed, apart from that the water recovery ratio was substantially increased for the case of crystallisation temperature lower than the eutectic temperature of NaCl.

As for the experiments on minimising the volume of the highly concentrated RO brines, the separation performance of a single-stage process was investigated with the sweating process. The results of the experimental investigation were highly encouraging, since the volume of the waste stream was reduced to a minimum level. Although the final product water of the SFC technology was not comparable with either drinking water or seawater standards (for some cases), the proposed process was able to further concentrate the highly concentrated RO brines as far as possible, while providing a significant amount of treated water, close to the quality of RO brine or seawater (for some cases). Based on the quality of the product water, the recommendation is for the treated water to be reused and recycled, either to join the main feed stream of a prior crystallisation process (i.e., falling film crystallisation and/or suspension crystallisation) or RO membrane plant.

Due to absence of appropriate experimental data in the literature, and the limited number of experimental runs (as presented in this study), the separation performance of the SFC process technology for water desalination applications, and more specifically RO brine concentration, should be further investigated. Since the parameters affecting the crystallisation and sweating processes were investigated within a limited range and number of experimental runs, carrying out further investigation with a wider range of parameters is highly recommended in future research. The suggested key parameters for the crystallisation tests are feed concentration, start and end-point crystallisation temperatures, crystallisation time, cooling rate, and average growth rate. The suggested key parameters for the sweating tests are the salt concentration of the crystal layer, sweating rate, sweating time, and the crystal mass ratio.

Acknowledgements

The authors would like to thank Sulzer Chemtech Ltd. for kindly supplying equipment and for their assistance during the pilot trials, particularly S. Dette, M. Stepanski, F. Lippuner and H. Engstler. The authors further acknowledge the support and guidance from Swansea University in participating and conducting this study. Also, the authors are thankful to the Director General of the Kuwait Institute for Scientific Research (KISR) and Executive Director of Water Research Centre, KISR for their support and encouragement towards this research.

References

[1] F. Melak, A. Ambelu, G.D. Laing, E. Alemayehu, Freeze desalination as point of use water treatment technology: a case of chromium(VI) removal from water, Proceedings, 2 (2018) 173.
[2] S. Lemmer, R. Klomp, R. Ruemekorf, R. Scholz, Preconcentration of wastewater through the Niro freeze concentration process, Chem. Eng. Technol., 24 (2001) 485–488.
[3] W. Gao, Y. Shao, Freeze concentration for removal of pharmaceutically active compounds in water, Desalination, 249 (2009) 398–402.
[4] G. Nebbia, G.N. Menozzi, Early experiments on water desalination by freezing, Desalination, 5 (1968) 49–54.
[5] W.E. Johnson, State-of-the-art of freezing processes, their potential and future, Desalination, 19 (1976) 349–358.
[6] A. Rich, M. Youssef, B. Nourimane, M. Denis, A. Souad, B. Christine, S. Naoual, K. Jean-Paul, B. Tijani, B. Ahmed, V. Stephane, Freezing desalination of seawater in a static layer crystallizer, Desalination, 13 (2010) 120–127.
[7] K.S. Spiegler, Y.M. El-Sayed, A Desalination Primer, Balaban Desalination Publications, Italy, 1994.
[8] M.S. Rahman, M. Ahmed, X.D. Chen, Freezing–melting process and desalination: review of present status and future prospects, Int. J. Nucl. Desalin., 2 (2007) 253–264.
[9] R.D.C. Shone, The freeze desalination of mine waters, J. South Afr. Inst. Min. Metall., 87 (1987) 107–112.
[10] M.S. Rahman, M. Ahmed, X.D. Chen, Freezing-melting process and desalination: I. review of the state-of-the-art, Sultanate of Oman, Sep. Purif. Rev., 35 (2006) 59–96.
[11] O. Miyawaki, L. Liu, Y. Shirai, S. Sakashita, K. Kagitani, Tubular ice system for scale-up of progressive freeze-concentration, J. Food Eng., 69 (2005) 107–113.
[12] E. Hernández, M. Raventós, J.M. Auleda, A. Ibarz, Concentration of apple and pear juices in a multi-plate freeze concentrator, Innovative Food Sci. Emerg. Technol., 10 (2009) 348–355.
[13] E. Hernández, M. Raventós, J.M. Auleda, A. Ibarz, Freeze concentration of must in a pilot plant falling film cryo-concentrator, Innovative Food Sci. Emerg. Technol., 11 (2010) 130–136.
[14] J.M. Auleda, M. Raventós, J. Sánchez, E. Hernández, Estimation of the freezing point of concentrated fruit juices for application in freeze concentration, J. Food Eng., 105 (2011) 289–294.
[15] J. Sánchez, E. Hernández, J. Auleda, M. Raventós, Freeze concentration of whey in a falling-film based pilot plant: process and characterization, J. Food Eng., 103 (2011) 147–155.
[16] J.E. Miller, Review of Water Resources and Desalination Technologies, SAND Report, Sandia Corporation, Sandia

National Laboratories, Albuquerque, New Mexico 87185 and Livermore, California 94550, 2003.
[17] OECD, Water Consumption. OECD Environmental Data Compendium, Organisation for Economic Co-operation and Development, 2004, pp. 136–137.
[18] J. Ulrich, H.C. Bülau, Melt Crystallization, Shaker Verlag, Germany, 2003.
[19] M. Ahmad, D.L. Oatley-Radcliffe, P.M. Williams, Can a hybrid RO-Freeze process lead to sustainable water supplies?, Desalination, 431 (2018) 140–150.
[20] P.M. Williams, M. Ahmad, B.S. Connolly, D.L. Oatley-Radcliffe, Technology for freeze concentration in the desalination industry, Desalination, 356 (2015) 314–327.
[21] https://www.sulzer.com/-/media/files/products/process-techology/processes-and-applications/brochures/suspension_crystallization_technology.ashx?la=en [Accessed on 12 June 2020].
[22] https://www.sulzer.com/-/media/files/products/separation-technology/crystallisation/brochures/fractional_crystallization_e.ashx?la=en [Accessed on 6 June 2020].
[23] O.K. Buros, ABCs of Desalting, 2nd ed., S.I. International Desalination Association (IDA), Topsfield, Massachusetts, United States of America, 2000.
[24] S. Lattemann, T. Höpner, Seawater Desalination: Impacts of Brine and Chemical Discharge on the Marine Environment, Balaban Desalination Publications, Italy, 2003.
[25] P.M. Williams, M. Ahmad, B.S. Connolly, Freeze desalination: an assessment of an ice maker machine for desalting brines, Desalination, 308 (2013) 219–224.
[26] J. Chang, J. Zuo, K.-J. Lu, T.-S. Chung, Freeze desalination of seawater using LNG cold energy, Water Res., 102 (2016) 282–293.